

Republic of Iraq
Ministry of Higher Education and Scientific Research
University of Al-Qadisiyah
College of Computer Science and Information Technology



Palm Vein Identification System Based On Convolution Neural Network

A Thesis

**Submitted to the Council of the College of Computer Science
and Information Technology at the University of Al-
Qadisiyah in Partial Fulfilment of the Requirements for the
Degree of Master in Computer Science**

By

Ali Salam Hameed

Supervised by:

Assist Prof. Dr. Ali Mohsin Mohammed

2021 A.D.

1443 A.H.

بِسْمِ اللَّهِ الرَّحْمَنِ الرَّحِيمِ

قَالَ الَّذِي عِنْدَهُ عِلْمٌ مِّنَ الْكِتَابِ أَنَا آتِيكَ بِهِ قَبْلَ أَنْ يَرْتَدَّ
إِلَيْكَ ظَرْفُكَ فَلَمَّا رآه مُسْتَقِرًّا عِنْدَهُ قَالَ هَذَا مِنْ فَضْلِ
رَبِّي لَيَبْلُوَنِي أَأَشْكُرُ أَمْ أَكْفُرُ وَمَن شَكَرَ فَإِنَّمَا يَشْكُرُ
لِنَفْسِهِ وَمَن كَفَرَ فَإِنَّ رَبِّي غَنِيٌّ كَرِيمٌ

صدق الله العظيم

سورة النمل آية 40

Supervisor Certificate

I certify that thesis entitled "Palm Vein Identification System Based on Convolution Neural Network" is prepared and written under my supervision at the Department of Computer Science / College of Computer Science and Information Technology / the University of Al-Qadisiyah as partial fulfillment of the requirements of the degree of Master in Computer Science.

Signature:



Assist Prof. Dr. Ali Mohsin Al-juboori

Date: / 11 / 2021

Head of Department Certificate

In view of the available recommendations, I forward the thesis entitled "Thesis Title" for debate by the examination committee.

Signature:




Dr. Qusay Omran Mosa


Head of the Department of Computer Science


Date: / 11 / 2021


Certificate of the Examination Committee


We, the undersigned, certify that (Ali Salam Hameed) candidate for the degree of Master in Computer Science, has presented this thesis entitled (Palm Vein Identification System Based On Convolution Neural Network) for debate examination. The examination committee confirms that this thesis is accepted in form and content and displays a satisfactory knowledge in the field of study based on the candidate demonstration during the debate examination held on: 10-November-2021.

Signature: 
Name: Suhad Ahmed Ali
Title: Prof. Dr.
Date: / 11 / 2021
(Chairman)

Signature: 
Name: Lamia AbedNoor Muhammed
Title: Assist Prof. Dr.
Date: / 11 / 2021
(Member)

Signature: 
Name: Qusay Omran Mosa
Title: Dr.
Date: / 11 / 2021
(Member)

Signature: 
Name: Ali Mohsin Al- juboori
Title: Assist Prof. Dr.
Date: / 11 / 2021
(Member and Supervisor)

Signature: 
Name: Dhiah Eadan Al-shammary
Title: Assist Prof. Dr.
Date: / 11 / 2021
(Dean of College of Computer Science and Information Technology)

Acknowledgments

Above all and after all, I must thank God for providing me with the strength to finish this study. All thanks to him, glorified and high, who gave me the right direction and courage to carry out this research work.

I express special thanks to Asst. Prof. Dr. Ali Mohsin Al-juboori, in addition to his valuable guidance and ideas for the completion of this work, I thank him for the interesting discussions and all the advice he gave to me, which included issues, guidance topics, useful discussions, comments, continuous encouragement, and support. I offer my sincere thanks and deep gratitude for those hours and the ideas he shared with me,

Special thanks to the Deanship of the college representation by Asst.Prof.Dr. Dhiah Eadan Al-Shammary for his support. Special thanks to all staff for their cooperation and the necessary facilities.

I would also like to express my deep gratitude and thanks to my family and all my friends for their unlimited patience in enriching my life and paving the course of science and knowledge.

Abstract

Biometrics is the biological measurements or physical characteristics that can be used to identify individuals. Recent research shed light on the use of classification algorithms based on biometric data to develop a new secure identification system or access-control mechanisms. A system that uses individual biometric features (usually an image), known as the unimodal biometric system and which relies on a single feature for identification. Therefore, this thesis proposes a single-media biometric system that uses biometric data (palm print recognition) to identify individuals. The purpose of the system is to build a strong biometric identification system that uses hand palm veins as attributes. The system consists of the biometric data pre-processing stage and classification stage using the Convolution Neural Networks (CNN).

To achieve this aim, images of the hand palm veins are required. The manual hand palm veins under the human body can be captured using infrared light (NIR) and the spectrum light of the camera to take it. The images must pass through several stages required for preprocessing which is necessary to produce a clear image for the manual hand veins pattern. The outputs images can then be used to extract patterns and compare them with the given characteristics to identify individuals based on the degree of similarity.

The refined image after the preprocessing steps must show the Region of Interest (ROI) which provides the meaningful data required for the training and matchmaking processes, hence an algorithm for ROI has been proposed. The algorithm will extract the pattern by first removing the boundary of the palm and separating it from the pattern vein so that the regime could not be accused of the fact that borders are part of the vein. Following ROI extraction, applying a few image filters, such as the state of the median filter, anisotropic filter, and closing operation system with background elimination, to allow the extraction of the veins clearly and facilitate the task for the CNN model. Thus, the CNN model

will take the output results of the pre-processing to perform the feature extraction, matching, and decision making. The model includes an input layer, hidden layers, and an output layer. The hidden layers include convolution layers, which play their role in the extraction of the features and the production of a map of features, the batch normalization layers to speed the training process, and ReLU for the activation layers.

The CASIA database for hand veins images has been used in this thesis. It contains 7200 images taken for 100 people in six different wave spectra, namely 900nm, 850nm, 700nm, 630nm, 460nm, and white color. Each person in the database has twelve images (each hand 6 images) of each wave spectrum. Hence, each band contains 600 images of the left hand and 600 images of the right hand. The whole dataset has been used. The images were divided into training and testing with three different ratios 50/50, 70/30, and 90/10 for training and testing respectively.

The results show that the higher accuracy was with a wave of spectrum 850nm because it has the ideal wavelength for extracting veins, hence it helps in developing an accurate model. The accuracy for left-hand palm veins was 97%, 97.5%, and 98%; and for the right-hand palm veins 96%, 97%, 99% according to the training/testing split ratios 50/50, 70/30, and 90/10, respectively. The results of the proposed model were benchmarked with AlexNet results that is a well-known global network trained on more than a million images; the proposed model excelled in terms of accuracy and time.

LIST OF PUBLICATIONS

Journals paper

1. A. S. Al-jaberi and a. M. Al-juboori, “palm vein recognition based on convolution neural network,” journal of al-qadisiyah for computer science and mathematics, vol. 13, no. 3, pp. Page–1, 2021.

Conference paper

1. A. S. Al-jaberi and A. M. Al-juboori, “palm vein recognition, a review on prospects and challenges based on casia’s dataset,” in 2020 13th international conference on developments in esystems engineering (dese), pp. 169–176, ieee, 2020.
2. A. S. Al-jaberi, A. M. Al-juboori, R. Al-jumeily, M. Al-khafajiy, and T. Baker, “Palm Vein Based Authentication System by Using Convolution Neural Network,” in 2021 14th international conference on developments in esystems engineering (dese), ieee, 2021 (Acceptable).

LIST OF CONTENTS

Chapter 1 - Introduction	1
1.1 Overview	1
1.2 Palm Vein Recognition	2
1.3 Related Work	3
1.4 Problem Statement	6
1.5 Thesis Aim and Objective	7
1.6 Use Case of Palm Vein Identification	7
1.7 Organization of Thesis	8
Chapter 2 – Theoretical Background	9
2.1 Introduction	8
2.2 Biometric System	8
2.3 Biometric System Phases	8
2.3.1 Enrollment Phase	9
2.3.2 Recognition Phase.....	9
2.3.2.1 Verification Mode	10
2.3.2.2 Identification Mode.....	10
2.4 Biometric Identification System	11
2.4.1 Image Acquisition Module.....	12
2.4.1.1 Vein of Palm Acquisition.....	12
2.4.1.2 Palm Vein Imaging Devices.....	15
2.4.1.3 Palm Vein CASIA Dataset.....	18
2.4.2 Preprocessing Module.....	19
2.4.3 Feature Extraction Module	21
2.4.4 Matching and Decision Module.....	22
2.5 Artificial Neural Networks (ANN)	23
2.5.1 The structure of Multi-Layer Perceptron (MLP)	23
2.5.2 Activation Functions	24

2.5.3	Loss Function	25
2.5.4	Back Propagation	26
2.5.4.1	Propagation Forward.....	26
2.5.4.2	Propagation Backward	26
2.6	Deep Learning Technique	26
2.6.1	Deep Neural Networks (DNN).....	27
2.6.2	Convolution Neural Networks (CNN)	28
2.6.2.1	Convolution Layers.....	28
2.6.2.2	Batch Normalization	29
2.6.2.3	Pooling Layers	30
2.6.2.4	Fully Connected Layers	30
2.7	Image Processing Techniques	31
2.7.1	Smoothing Spatial Filter	31
2.7.1.1	Smoothing Linear Filter	31
2.7.1.2	Smoothing Nonlinear	32
2.7.2	Image Segmentation.....	35
2.7.3	Morphology Operation.....	37
2.7.3.1	Dilation.....	38
2.7.3.2	Erosion	39
2.7.3.3	Opening.....	40
2.7.3.4	Closing	40
2.7.3.5	Boundary Extraction	40
2.8	Performance Measures	41
2.8.1	Confusion Matrix	41
2.8.2	Sensitivity (Se):	42
2.8.3	Specificity (Sp):	42
2.8.4	Precision (Pr):	42
Chapter 3 - Design principles and preparation.....		43
3.1	Introduction	44
3.2	Proposed System	44
3.3	Image Preprocessing	46

3.3.1	Preprocessing Stage for Palm Vein.....	46
3.3.2	Palm Vein Region of Interest (ROI)	46
3.3.2.1	Image Rotation.....	47
3.3.2.2	Binarization.....	48
3.3.2.3	Noise-Removal.....	49
3.3.2.4	Boundary Extraction	50
3.3.2.5	Determination the joint points of the palm.....	51
3.3.3	Enhancement image of the region of interest.....	53
3.4	Pattern Extraction.....	55
3.5	Feature Extraction	56
3.5.1	Palm Vein Identification System Based on proposed CNN	57
3.5.1.1	Convolution Layer (Conv)	59
3.5.1.2	Batch normalization layers (BN)	60
3.5.1.3	Rectified Liner Activation Function (ReLU).....	61
3.5.1.4	Average Pooling Layer (AP).....	62
3.5.1.5	Fully Connected Layer (FC)	63
3.6	AlexNet.....	64
3.7	Matching and Decision	65
3.7.1	Softmax Layer.....	65
3.7.2	Loss function.....	66
Chapter 4 – Experimental result and discussion of the proposed system.....		67
4.1	Introduction.....	67
4.2	System Requirements.....	67
4.2.1	Hardware Requirements.....	67
4.2.2	Software Requirements	68
4.3	Test and Implementation.....	68
4.4	Dataset.....	68
4.5	Experimental Result of the Proposed System.....	70
4.5.1	Preprocessing Stage	70
4.5.2	Convolutional Neural Network (CNN).....	72

4.5.2.1	Feature Extraction	72
4.5.2.2	Matching and Decision	73
4.6	Training and Test Validation	73
4.7	Result and Discussion of Palm Vein Identification Based on proposed CNN	74
4.8	Result and Discussion of Palm Vein Identification Based on AlexNet	80
	Chapter 5 – Conclusion and future direction	88
5.1	Conclusion	85
5.2	Future Directions	86
	References	87
	Appendix A	93
	Multiple Spectral Image Details	93

LIST OF FIGURES

Figure (1.1) Extract vein pattern from the palm (a) Visible ray image (b) Infrared ray image (c) Extract vein pattern [7]	3
Figure (2.1): Block diagram shows the Enrollment Phases [19]	9
Figure (2.2): Block diagram shows as the (a) Verification (b) Identification [19].....	11
Figure (2.3): Diagram showing the main steps for recognition of personal using vein of palm images	14
Figure (2.4): Diagram showing of the light through layers of skin [27]	14
Figure (2.5): capturing the image of palm vein methods (a) Method of refraction (b)	19
Figure (2.6): The structure of Multi-Layer Perceptron (MLP).....	23
Figure (2.7): Abstract of Deep Neural Network diagram [49].	27
Figure (2.8): Example of convolution layer.....	29
Figure (2.9): Example of average pooling	30
Figure (2.10): Example of median filter	33
Figure (2.11): Otsu method [67]	37
Figure (2.12): Dilation process	38
Figure (2.13): Erosion process.....	39
Figure (2.14): Boundary extraction	41
Figure (3.1): The diagram of proposal system.....	44
Figure (3.2): Rotation method (a) The original image (b) Image after rotate	47
Figure (3.3): Otsu method (a) The rotate image (b) Image after Otsu threshold.....	48
Figure (3.4): Opening operation (a) image after Otsu threshold (b) Noise Removal after opening morphological operation	62

Figure (3.5): Extraction boundary (a) Noise Removal after opening morphological 63
Figure (3.6): The diagram of important point in palm.....	51
Figure (3.7): Median filter (a) The region of interest (b) The ROI after median filter...	53
Figure (3.8): Anisotropic filter (a) The ROI after the median filter (b) The ROI after Anisotropic diffusion filter 51
Figure (3.9): Closing operation (a) The ROI after Anisotropic diffusion filter (b) The ROI after closing morphological operation.....	69
Figure (3.10): Extraction pattern (a) The ROI after closing morphological operation (b) Extraction pattern of vein70
Figure (3.11): The layer of proposed Convolution Neural Network 57
Figure (3.12): Proposed CNN Architecture for palm vein recognition 58
Figure (3.13): The Architecture of AlexNet 64
Figure (4.1): Multispectral imaging device 69
Figure (4.2): six image of Palm print from dataset.....	69
Figure (4.3): Figure (4.3): Show as the step of preprocessing stage (a) The original image (b) Rotation image (c) Binary image (d) Noise removal (e) Boundary extraction (f) Determine ROI (g) ROI extraction (h)extraction pattern 88

LIST OF TABLE

Table 2-1 Comparison of palm vein image technologies and devices	16
Table 2-2 CASIA dataset.....	19
Table 2-3 Location of ROI in literature	21
Table 3-1 The details of this layer	59
Table 3-2 The details of AlexNet.....	64
Table 4-1 Split of database image.....	74
Table 4-2 the analysis result of our proposed CNN.....	75
Table 4-3 Details information of data training about 850L using proposed CNN	76
Table 4-4 Accuracy of the band 460 nm.....	76
Table 4-5 Accuracy of the band 630 nm.....	77
Table 4-6 Accuracy of the band 700 nm.....	77
Table 4-7 Accuracy of the band 850 nm.....	77
Table 4-8 Accuracy of the band 940 nm.....	78
Table 4-9 Accuracy of the band WHT nm	79
Table 4-10 Accuracy of all data.....	79
Table 4-11 Details information of data training about 850L using AlexNet.....	80
Table 4-12 Accuracy of the band 460 nm.....	81
Table 4-13 Accuracy of the band 630 nm.....	81
Table 4-14 Accuracy of the band 700 nm.....	81
Table 4-15 Accuracy of the band 850 nm.....	82
Table 4-16 Accuracy of the band 940 nm.....	82
Table 4-17 Accuracy of the band WHT nm	83
Table 4-18 Accuracy of all data.....	83

LIST OF ALGORITHMS

Algorithm 3-1 Otsu threshold	49
Algorithm 3-2 Extraction ROI.....	52
Algorithm 3-3 Batch normalization.....	61
Algorithm 3-4 Activation function ReLU	62
Algorithm 3-5 Average pooling.....	63

LIST OF ABBREVIATIONS

AI	Artificial Intelligent
AlexNet	Alex Network
ANN	Artificial Neural Networks
AP	Average Pooling
batch Nrm1	Batch Normalization
<i>BN</i>	Batch Normalization
CASIA	Chinese Academy of Sciences Institute of Automation
CCD	Charge Couple Device
CNN	Convolution Neural Network
Conv	Convolution
<i>DL</i>	Deep learning
DNA	Deoxyribonucleic Acid
DNN	Deep Neural Networks
<i>FC</i>	Fully Connected
FER	False Error Rate
F-S	F-Score
ICA	Identification component analysis
Jpeg	Joint Photographic Experts Group
LED	Light Emitting Diode
MLP	Multi-Layer Perceptron
NIR	Near Infrared
PCA	Principle Component Analysis

Pr	Precision
RAM	Random Access Memory
ReLU	Rectified Liner Activation Function
ROI	Region of Interest
Se	Sensitivity
Sp	Specificity
VGA	Video Graphic Array
VGGNET	Visual geometry group network

Chapter 1 - Introduction

Chapter One

Introduction

1.1 Overview

Previously, people used the password and personal identification number for security purposes, recording entry into their bank account, credit card, and telephone. However, passwords and personal identification numbers could be forgotten and lost. If they were kept anywhere, they would be at risk of theft by criminals or identity bandits through a false page, Trojan application to avoid such vulnerability, biometric features are used [1].

Biometrics is a science or technique to measure the unique physical and behavioral characteristics of each individual and mean measurements of individual advantages, such as fingerprints, that can identify or verify the person. Using this method, biometrics is a password that cannot be forgotten, lost, or stolen [2].

There is much possible biometrics, including Deoxyribonucleic Acid (DNA), smell, walking, long, handwriting, and speaking, but vision-based biometrics use image sensors and algorithms derived from the vision of the machine. Biometrics contain some associated safety standards, the first biometrics cannot be copied, the second can be lost only in the event of an accident, the third depends on the uniqueness of human characteristics and the biometric advantage cannot be shared because it is linked to the individual [3].

Biometric features are divided into physical features such as handprint, iris, hand geometric, etc., and behavioral features such as key

pressure. Each of these features has positive and negative features, for example, a fingerprint that has high accuracy but cannot be acquired for sugar patients, and there are concerns about the transmission of leather diseases. To avoid this, in addition to the above-mentioned problem, access to photographs is used to facilitate the recording of the user entry and/or verification. At present, many people use one of these physical or behavioral features, such as fingerprint, handprint, voice, finger vein, face, etc., in their markets or company. One feature is called the unimodal biometric system, which is usually used for security purposes, but the single media system is not strong and fully established. All unimodal biometric systems have their advantages and disadvantages [4] to overcome the weakness (defect) of the one-system method. More than one biometric feature is linked/ Ownership of performance in large database applications [5].

1.2 Palm Vein Recognition

The academy and foundation have tried to develop a device that can identify under blood vessel patterns. Fujitsu developed a palm vein technique using cardiovascular patterns as personal identification data [6].

Identification of palm vein uses individual port radiation patterns as personal identification data as shown in figure (1.1). Compared to the finger or hand, the hand vein has wider and more complex, and therefore contains a wealth of characteristic features of personal identification. The palm vein technique is safe because validation data are in the body and therefore very difficult to falsify. This technology has many applications such as banks, hospitals, and government offices, issuance of passports, libraries, and personal computers. Business growth will be achieved through these

solutions by reducing the size of the palm gallery and shortening the time of validation [7].

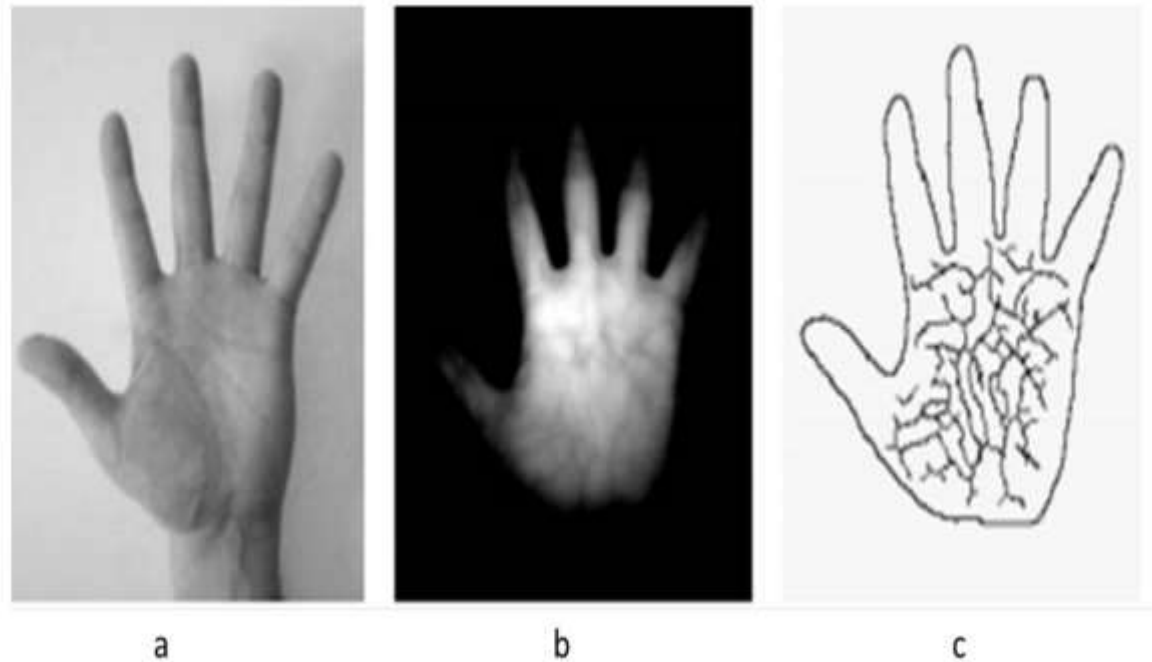


Figure (1.1) Extract vein pattern from the palm (a) Visible ray image (b) Infrared ray image (c) Extract vein pattern [7]

1.3 Related Work

Goyal, M in 2011 [8]. provided an in-depth overview of the principles and applications of morphological analysis, through a systematic process from the underlying morphological factors to the latest developments that proved to be of practical utility. This technique has shown that morphological concepts constitute a powerful set of tools to extract features that matter to the image and a great advantage in terms of implementation has shown that extension and erosion are primitive processes.

Ray et al in 2013 [9]. the region of interest extraction approach is based on the principle of choosing an area where rich textile patterns can be found. The image acquired has been divided into smaller horizontal and vertical tapes and the statistical characteristics of these areas have been used to either determine or reject the edges from the return on investment. Histogram techniques are used to verify the suitability of the extracted region.

Yogamangalam et al in 2013 [10]. provided a brief outline of some of the most common segmentation techniques such as threshold, model-based, clustering, and edge detection. Mention her advantages and disadvantages. They summarized the different segmentation techniques. This division was made to estimate the surfaces. This has proved that, compared to other methods, the threshold is faster and simpler.

Ahmed et al in 2013 [6]. Provide algorithm analysis, techniques, methodologies, and systems for identifying disfigurements. They discussed some technical aspects of ROI approaches to detecting post-processing returns, dividing the palm vein pattern, extracting features, and matching. Their results show that there is no reference database to identify palm veins. For all operations, there are many very high accurate automated learning techniques.

Matta, S in 2013 [11]. Discussed the various segmentation techniques available, outlining the advantages and disadvantages of these different techniques, where different factors are affecting the process of fragmentation of the image, such as image homogeneity, spatial characteristics of continuity of the image, touching, and content of the image.

Bhosale et al in 2014 [12]. three different algorithms were used to address the images of the palm vein pattern of an individual captured by CCD CAMERA. This processed picture will be used later to validate the person. Biometric algorithms are used for human identification consisting of validation, recognition, and verification.

M. Rajalakshmi et al in 2017 [13]. CNN was used to validate the backpack pattern, the region of interest extracted using the use of contour and edge detection. The four-tiered CNN structure was then proposed to identify the palm dorsal. A 50-person palm vein database was used with five samples per subject for system experiments with a 98% accuracy rate. 80/20 percent for training and test samples, respectively.

D. Thapar et al in 2019 [14]. propose a new way to design an end-to-end deep CNN framework i.e., PVSNet that works in two major steps: first, an encoder-decoder network is used to learn generative domain-specific features followed by a Siamese network in which convolutional layers are pre-trained in an unsupervised fashion as an autoencoder. The proposed model is trained via triplet loss function that is adjusted for learning feature embeddings in a way that minimizes the distance between embedding pairs from the same subject and maximizes the distance with those from different subjects, with a margin. In particular, a triplet Siamese matching network using an adaptive margin-based hard negative mining has been suggested. The hyper-parameters associated with the training strategy, like the adaptive margin, have been tuned to make the learning more effective on biometric datasets. In extensive experimentation.

S. Chantaf et al in 2020 [15], proposed was done on a palm vein database that was taken at the University of Lebanon, Faculty of Technology,

Saida, where the data contained 4000 images. 100 samples were taken from the left and right hands of 20 people, 8 females and 12 males. They trained using deep learning. After extracting the pattern of the veins in a process before treatment. They were entered into the google net and the VGGNET network, where the results were as follows. For VGGNET in the case 50/50 82.5% and the case 75/25, the accuracy is equal to 85% and in the case 80/20, the accuracy is 93.2% As for the case. For the GoogLeNET network, it was as follows, when the case was 50/50, the accuracy was 80%, and in the case 75/25, it was 82% and in the case 80/20, it was 91.4%.

S. Y. Jhong et al in 2020 [16], proposed a modified convolutional neural network to determine the best recognition model through training and testing. Finally, the developed system was implemented on the low-level embedded Raspberry Pi platform with cloud computing technology. The results showed that the system can achieve an accuracy of 96.54%.

1.4 Problem Statement

Many of the problems that have arisen in biometric methods have led to many constraints, such as:

1. In a variety of biometrics, the problem lies in the changes that occur in the body. When a person changes a lot with age and body expressions at each time, there is a need to establish a data set of unstable form and continuous changes. This requires huge data and this is a problem.
2. Region of interest algorithms is limited, as they operate on a specific data set.

3. In the most common identification systems, the training process is slow, resulting in a relative slowdown in the entire system.
4. The database that was used in this thesis has images taken with more than one wavelength spectrum, and this is a problem in extracting the patterns because the pattern of veins is clear between the 700nm-900nm wave spectrums.

1.5 Thesis Aim and Objective

The purpose of this thesis is:

1. Solving the security issues and identification problems.
2. The growth of using technology has increased day by day, therefore how can protect the privacy and save user data.
3. Building a strong system for identifying biometrics that relies on its palm vein based on deep learning.
4. Increased speed of training (time-saving) using the proposed CNN module.

1.6 Use Case of Palm Vein Identification

Palm vein has been used in a variety of applications such as door safety systems, computer access management systems, financial services, payment services, and hospital identification systems. The pattern of the hand has a two-dimensional complexity, and because the picture is under the skin, the acquired picture is very constant. Building on these advantages, that the ratification of the palm vein will be widespread.

1.7 Organization of Thesis

The thesis was organized as follows:

Chapter Two: This chapter begins with a short introduction to the processing of images and to identify patterns. It then explains the methods used for the extraction of advantages and provides the measure of distance used in the classification.

Chapter Three: This chapter describes the steps designed for the entire system and describes all algorithms used to implement the system.

Chapter Four: This chapter presents the results of the implementation of the experiments and discusses the results obtained.

Chapter Five: the conclusion from the proposed system and some recommendations made to strengthen the work proposed in this chapter.

Chapter 2 – Theoretical Background

Chapter Two

Theoretical Background

2.1 Introduction

Chapter two provides an overview of the methods and mechanisms used to conduct the process in the biometric system in the palm vein, starting with biometric image acquisition, preprocessing, and operation of the region of interest, pattern extraction, extraction of feature, and matching feature. In addition, detailed descriptions of convolution neural networks (CNN) and performance measurement tools follow it.

2.2 Biometric System

Biometrics is the technical term for body measurements and calculations. Referring to human character measurements. The validation of biometrics (or realistic validation) in computer sciences is used as a form of identification and access control [17].

Biometrics is essentially the typology system that obtains biometric data from the individual's character, extracts a set of features for training the system. There are two types of features, physical features that mean the nature of the human body or behavioral features that depend on individual behavior, the trained system will be ready to perform personal identification or verification [18].

2.3 Biometric System Phases

Generally, the biometric system consists of two basic phases:

2.3.1 Enrollment Phase

At this stage, biometric data are obtained through sensors and special devices used for this purpose, such as cameras and scanners. The data collected then moves to advance processing for improvement and extraction of the region of interest. Then, through the process of extracting the pattern, the feature that will represent the person's extraction, the feature extracted in. finally, the extracted features are stored in the database [19]. Figure (2.1) shows the Block diagram of the Enrollment Phase.

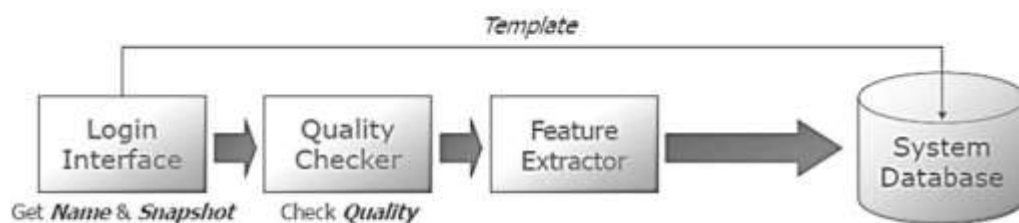


Figure (2.1): Block diagram shows the Enrollment Phase [19]

2.3.2 Recognition Phase

Biometric data captured from the registered person at the identification stage, and these biometric data advanced through the same stage of preprocessing, pattern extraction, and extraction of features, in addition to the process of comparing the combined (acquired) feature with the corresponding feature previously collected and stored in the database, for

identification. Identity management functions include two identification and verification methods [19] [20].

2.3.2.1 Verification Mode

The phase of verification is one identical process, in which case the person requests an identity that is usually known, named and a user name ...etc. the system compares the person's feature, which has been appointed, with only one set of features that corresponds to its identity. A person is accepted or refused based on the degree of similarities between these two groups of features [17].

2.3.2.2 Identification Mode

The identification works in the same manner as the verification status, but it is an individual reconciliation process for more than one person since the person does not request an identity. The system has to identify the person by scanning the benefit collections of all trained users (registers) in the system's reconciliation database (or fail, give a warning when the person is not registered. The purpose of the definition is to avoid a person (one individual) from using multiple identities for the rest (the user does not prefer to request an identity). Figure (2.2) provides the biometric registration scheme and (verification and definitional conditions).

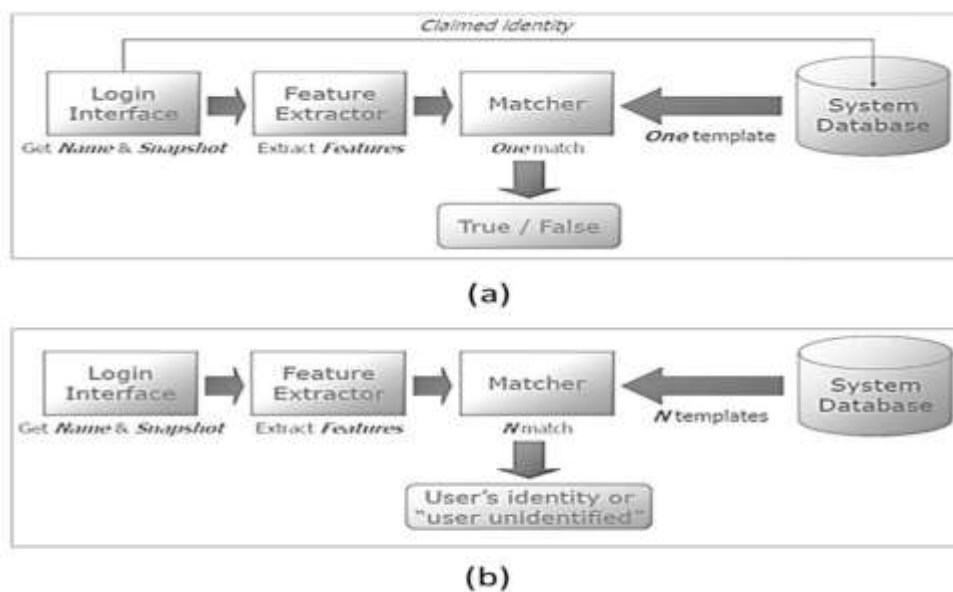


Figure (2.2): Block diagram shows as the (a) Verification (b) Identification [17]

2.4 Biometric Identification System

Palm vein is one of the most interesting types of biometric techniques. It is almost like a palm print, but instead of using the visual light spectrum to take a hand fingerprint, the vein needs the nearest infrared lighting (NIR) to capture the vein pattern because it falls under the back skin of the hand. Every person has unique in-home characteristics that can be used for identification or verification. Compared to other biometric techniques, the vein is [19]

- A. Less expensive.
- B. Accessibility.
- C. Given the presence of the grid within the human body, it is difficult to counterfeit or change.

The handprint is one of the most important biometric features used for identification since it is uniquely based on the baseline, permanent incisive status, and other features such as the exact details in the contact position [20].

The biometric recognition system is generally composed of four main modules: the Image Acquisition Module, preprocessing module, feature extraction module, feature machining, and the Decision module [2].

2.4.1 Image Acquisition Module

The first step in each biometric identification system is the acquisition of data (image), where the Image Acquisition Unit acquires the photograph of raw biometrics from individuals (e.g. Palm). In the acquisition module, a specific multi-spectral palm camera was used, using NIR, which reliably penetrated the skin depth, lit the infrastructure, and traps the ice based on its temperature. Near-infrared light is not harmful, safe, and relatively inexpensive [20] [21]. A visual light shall use with an appropriate camera and sometimes used to limit the location and direction of the hand to obtain a palm without contact [22].

2.4.1.1 Vein of Palm Acquisition

In the acquisition of image stage, the images in the CASIA dataset that was the acquisition by the Charge Couple Device (CCD) camera were used. In addition, the preprocessing stage includes selecting the important area of the palm. Where there are areas that are not necessary and do not need it, so choose the important part of the palm and this area is called the region of interest (ROI) which includes several stages, which consist of noise removal,

binarization, boundary extraction, determining the joints, and drawing rectangle around ROI. When the ROI zone is finished, an image enhancement stage comes which includes stages, and then comes a segmentation stage, which also contains several stages. Feature extraction obtains high-quality factors from the pre-processing veins of the palm. An electronic matching compares two veins of palm elements and dataset retail the resulted in registered templates [23]. Figure (2.3) shows the Diagram of the main steps for the recognition of personal using vein of palm images.

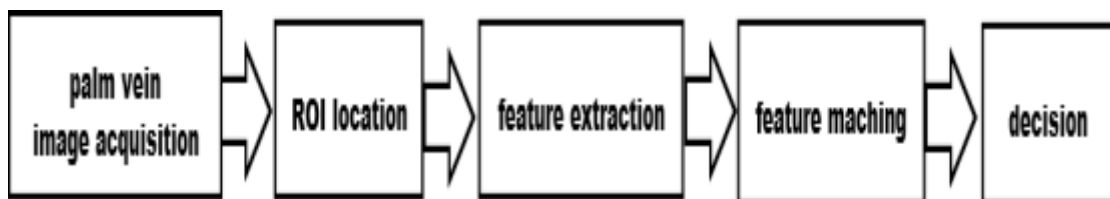


Figure (2.3): Diagram showing the main steps for recognition of personal using vein of palm images

This leads us to the principle of the vein of palm imaging the scientific spectral window (700-900)nm should to Near Infrared (NIR) absorption of the hemoglobin collectively with the oxygen of containing hemoglobin and deoxidizing hemoglobin in the vein of palm vessels is more powerful than the close to NIR absorption of the web that is around it [23]. When the infrared light enters the palm, the oxidizing blood vessels absorb it and form the shade. There are three layers of content skin of the palm. The most external epidermis-dermis and the layer of subcutaneous as illustrated in figure (2.4). The stratum conium overlay out of doors of the skin of the palm consists of the lifeless skin cells and is epidermis section.

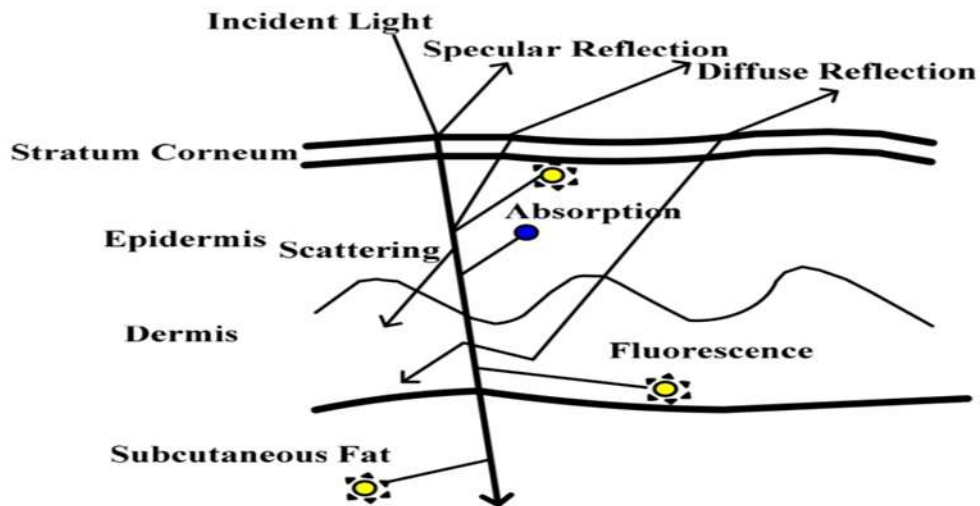


Figure (2.4): Diagram showing of the light through layers of the skin [2]

After the dermis layer of the skin, there is the subcutaneous layer that will reflect the rest of the skin layers. NIR will absorb the light that is on it and reduce the light that causes light scattering but the rest of the light in this case will not be able to move deep down the skin layers. It is more estimated to have a higher resolution for the palm vein when the imaging process is done. Reflection and transmission are the main ways or methods in imaging the palm vein in which are shown in figure (2.5). The first one, reflection, focuses the light on the front of the palm. The second one, transmission focuses the light on the back part of the palm. It needs a very high quality light to be transmitted through the skin, in many uses it can be used closely with the skin of the palm.


















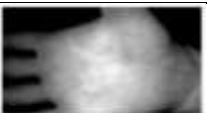








Figure (2.5): capturing the image of palm vein methods (a) Method of refraction (b) Method of transmission [2]

2.4.1.2 Palm Vein Imaging Devices

The capability of capturing the palm image is the core rock of the process of palm vein recognition. CCD device is used in palm vein recognition. it is used with a certain type of light called LED to capture the palm vein photo to give an exact result about the personal data or the secured data of that person, using infra-red images to show the finger or palm vein pattern is considered a promising step into the new postmodern biometrics technology advancement. In addition, the main process of this technology is remote scanning which means less touching area and more convincing results and more convincing social security to the user as mentioned before. 3mm is where our image of blood vessels where to be captured, the infra-red LED is used in the normal way which is the close illumination either in the reflection method or in the transmission, and the image is usually captured by a CCD camera that has a certain kind of filter that recognizes only this kind of light. With the authentication process, NIR light was used to show the exact palm veins with no need for touching the sensor and leaving marks that can be used again because it is a light technology and it is proving our point in the privacy policy. Scanners and digital cameras capture palm vein images, that the thing that attracted most researchers to look more into this process. Moreover, a set of optical gadgets work together in precise harmony to acquire the exact network of our blood micro tubes it traces blood flowing which is wherever there is hemoglobin in the vessels by a high-resolution camera [24]. Table (2.1) shows some devices to capture palm vein images.

Table 2-1 Comparison of palm vein image technologies and devices


Literature	Capture device	Sample of image	Camera type	Light source	Image method
[25]			CCD camera	A set of infrared light	Reflection
[26]			CCD NIR camera (JAI AD-080 CL 1/3'')	850nm LED arrays	Reflection
[27]			Webcam	880nm to 920nm infrared LEDs	Reflection
[28]			CCD camera	850nm IR LEDs	Reflection
[29]			Low-cost USB camera	880 IR LED	Reflection
[30]			CCD camera (Sony XC711)	LED infrared peak at 750nm	Reflection

[31]			CCD camera (Sony ICX618)	940nm LEDs	Reflection
[32]			CCD camera	LEDs 850nm	Reflection
[33]			NIR camera	850nm 30nm LED	Reflection
[34]			CCD camera (IEEE 1394 Sony ICX618)	940nm NIR LEDs	Reflection
[35]			Infrared night-vision camera (Zmodo zb-ibh 13)	850nm LEDs	Transmission
[5]			CCD camera	Near IR LEDs (SFH4550) 850NM matrix	Transmission

2.4.1.3 Palm Vein CASIA Dataset

The act of recognition is a wide process and it is open to continuous change in the concept of the electronic and digital world. No denial in mentioning that it faced some drawbacks in time, accuracy, and cost, but somehow it managed to control the needed market and to produce the most suitable gadgets to perform the process of recognition in a good way. CASIA is a massive palm print database that deals with multi-spectral recognition and capturing the palm vein images and develops many other modalities in biometrics. This database contains a huge number of palm vein images, using optical and spectral devices to capture the image as accurately as possible. Moreover, it uses the session's system at different wavelengths for the same light source [940nm, 850nm, 700nm, 630nm, 460nm, and normal white light], each hand has six images, and with different postures to get this accurate network of blood vessels, the time between sessions could be 30 days [36]. However, diversity is the goal of this difference in time, postures, and light frequency, this CCD camera is fixed automatically to capture six images of each hand posed in front of the one-colored background also with no need to put any restrictions on the user of the palm vein identifier. Table (2.2) shows the CASIA dataset

Table 2-2 CASIA dataset

CASIA multi spectral palm print image dataset	
Palm number	2700
Sample number	6
Wavelength or light	940nm,850nm,700nm, 630nm, 460 nm and white
Camera type	CCD camera
Image size (pixel)	768*576
Example	 850nm

2.4.2 Preprocessing Module

Preprocessing stage is the basis for extraction feature and matching as the accuracy of the system depends on the quality of the pre-processing, which has a major impact on the recognition results. Region of interest is an important stage in preprocessing apart from other measures such, filtering, enhancement of image, etc.

The region of interest extraction approach includes five significant steps:

- A. Rotation of the original image.
- B. Binarization of the image of palm.

C. Noise Removal.

D. Boundary Extraction.

E. Determine the joint points of the palm.








There are numerous unique implementations, as tested in table (2.3) region of interest strategies account for the manageable scale modifications in the contactless palm vein recognition. The place of the region of interest used to extraordinarily particularly base on two textures, the internet between the index finger and core finger collectively with the internet between the finger of the ring and little finger, as confirmed in the table (2.3) [30][31]. They locate the two textures by discovering the conformable close by minima from the calculated distance [37].

Several works of literature derived the region of interest extraction approach from palm print recognition. While this region of interest strategies consist of three principal strains of palm print, which form faked, information of palm vein. The preprocessing algorithm section rectangular areas for characteristic extraction for the square region is easier for managing translation variation, whilst the half and circular of elliptical areas can additionally be simpler for handling rotation variation. Several works of literature on palm print recognition used round or half of the elliptical areas as their region of interest. Possibly the contactless vein of palm focus has a try. Contactless vein of palm region of interest vicinity is nonetheless a challenge. It did a lookup on finding the region of interest when the rotation of the user's hand is massive and grew to become round to sure angles [30].

Palm vein recognition is first known in 1991 the palm vein cannot be easily captured and because of this, it is classified as a high of security human recognition for no palm vein is copied or even inherited in genetic relations[38].

The blood flowing in the veins is what makes the palm vein recognition is possible to sense the palm vein it does not need direct contact with the electronic sensor even with some external effects like water, mud, oil, or even plastic gloves all this will not affect the recognition results [38].

Table 2-3 Location of ROI in literature

Literature	Location of ROI
[23]	
[2]	
[39]	
[40]	
[41]	
[27]	
[42]	

2.4.3 Feature Extraction Module

Extraction of feature is the process of drawing interest and certain prominent features that are the key feature of the biometric pattern called the template, play an important role in identification systems because of the use

of the resulting representation as an input to the identification process and thus affect mainly the product of the matching process.

The biometric system has several ways to extract biometric advantages. Some of these methods focus on the local details of the specifics of the wet, while others offer a global representation of palm information such as the baseline. A number of extraction methods below [21] [22].

1. Geometric-based: This method relies on Geometrical information such as sites, patterns, long ages, facts, or forms of biometric features.
2. Texture-based: This method relies on the fabric information of the biometric image for the representation of the print reference template (in palm print, fingerprint).
3. Appearance-based: usually used to extract a palm feature. This method can be operated through algorithms (PCA, LDA, and ICA) [43].

2.4.4 Matching and Decision Module

The matching and decision module at times allowed to like the arrangement module on the most proficient method to coordinate the biometric highlights acquired with those generally put away in the data set. There are numerous techniques utilized for the matching and Decision module, like Hamming Distance, intelligent administrators, for example, administrators XOR, AND, as well as, histogram intersection distance, Euclidean distance, and smart class (application of artificial neural network ANN and artificial intelligence AI). Notwithstanding, the decision relies upon the similarity of strategies with the component of the vein and their portrayal. The level of similarity was passed to the choice module, which utilizes the limit for the order of the picture taken [43] [21].

2.5 Artificial Neural Networks (ANN)

Artificial neural networks are several interconnected computational contracts. ANN is a computational approach to problems in which adequate representation is found to solve the problem; it is difficult for traditional computer programmers. Artificial neural networks are sometimes referred to as boxes black because it was impossible to understand their work (function) [36].

2.5.1 The structure of Multi-Layer Perceptron (MLP)

The Structure Multi-Layer Perceptron (MLP) It is a forward feeding structure for artificial neural networks containing one or more hidden layers, and each layer consists of a simple, mathematically connected combination of the contract known as neuro cells as shown in figure (2.6) [44] [45].

Each neural in each hidden layer and product layers are connected to all neuro cellular cells in the former layer, and all connections have an attached weight, representing the strength of neurological communications [46].

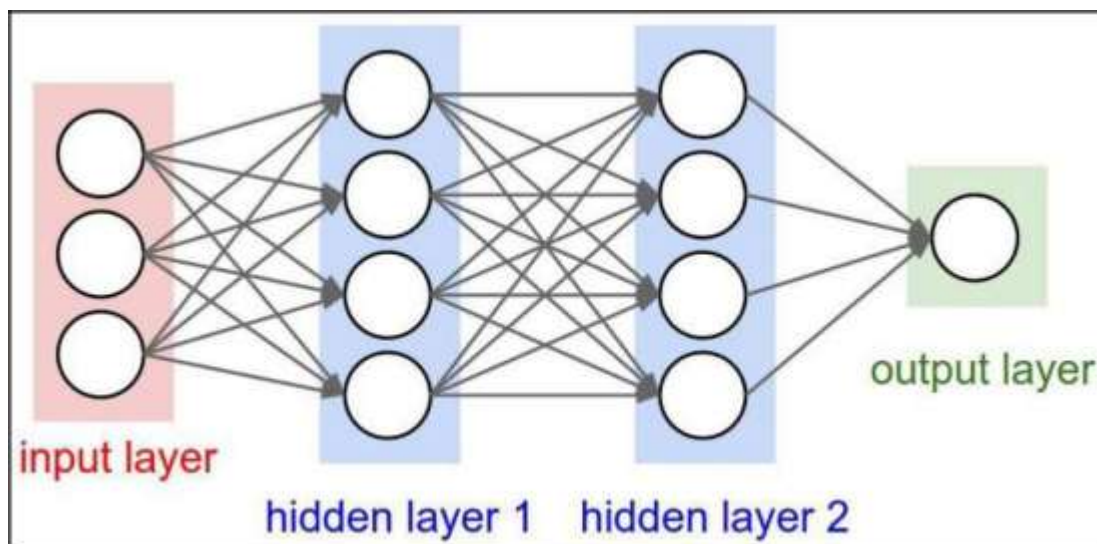


Figure (2.6): The structure of Multi-Layer Perceptron (MLP)[46]

The value of the output is described for each j neural cell in layer l in equation (2.1) [45] [47].

$$z = \sum_i^N (W_{i,j} \cdot X_i) + b \quad (2.1)$$

Where N is the input number, i.e. inputs that passed from (l-1), ($W_{i,j}$) are the weight of the edge linking the neural of the presentation layer with the neural of the former layer, and (b) like bias, the equation (2.1) is written in simplified matrices to be as follows [43] [48] :

$$Z = W^T x + b \quad (2.2)$$

2.5.2 Activation Functions

This function is to be determined, as the neuro cell should be activated or not activated by calculating the total weight and addition with bias. The main purpose of using the activation function is to give the irritation to extract nervous cells, for learning and carrying out complex tasks. Back Propagation makes it possible the most active function used is the corrected written unit (ReLU), and the equation (2.3) illustrates the representation of the ReLU.

$$O(x) = \max(x, 0) \quad (2.3)$$

The output layer needs to assess the probability of individual categories. For this reason, softmax is the most common activation function used to equate the output layer (2.4) Clarify this function.

$$O(x) = \frac{e^{x_k}}{\sum_j e^{x_j}} \quad (2.4)$$

Where X_k the corresponding production of category k and j is the total number of classes [44] [45] [49].

2.5.3 Loss Function

The loss function is used in the neurological network to estimate the prediction of error there are different types of loss functions such as cross-entropy and mean square error, and this method is used in Neural networks for multiple categories using softmax.

$$L = \frac{1}{n} \sum_{k=1}^n \ln o(x^k) + (1 - z^k) \ln (1 - o(x^k)) \quad (2.5)$$

Where "n" represents the number of categories, " z^k " is the required output of category k, while " $o(x^k)$ " is the estimated probability of category k, calculated using the SoftMax activation function described in the equation (2.4) [45] [49] [50].

In the MLP layers, weight edited (adjusted) during training, the back propagation algorithm is the most common algorithm used to control weight in the training process.

2.5.4 Back Propagation

Back propagation is a supervised learning calculation that is broadly utilized in the preparation of the neural organization, given its effective and straightforward design. Back proliferation utilizing the extents strategy to diminish neural networks error. At the beginning of the training process, weights and biases are set up in the network with a random number, and there are two phases of counter-proliferation [44] [51].

2.5.4.1 Propagation Forward

The Input case is spread toward the whole network. Layer by layer starting from contribution to yield utilizing condition (2.1) and condition (2.3) to deliver expectation esteem.

2.5.4.2 Propagation Backward

Backward the second part of the forward end, which begins with the calculation of the error and the propagation of a layer after another from outputs to inputs, and the weights and biases are updated accordingly. To do backward propagation, a job that continues with derivatives is required. There are two types of active posts based on the type of appointment required from entry to graduation. The first is a nonlinear function such as sigmoid, and the second type of activation function is the liner function (ReLU) explained in equation (2.3). When these stages are repeated all inputs. This is called an epoch. The NN can run for some epoch, as it is needed to discover its Arrangement [52].

2.6 Deep Learning Technique

Deep learning is a category of automated learning algorithms that use multiple layers to extract advantages with a gradually higher level of initial

inputs. For example, in image processing, lower layers may determine the edges, while the upper layers may determine human-related concepts such as numbers, letters, or faces. This process is carried out through successive layers that further complicate the steps taken. Each product layer. It passes as an entrance. The next layer is used to learn the features of the high level (the most complex), as explained. Figure (2.7) [47].

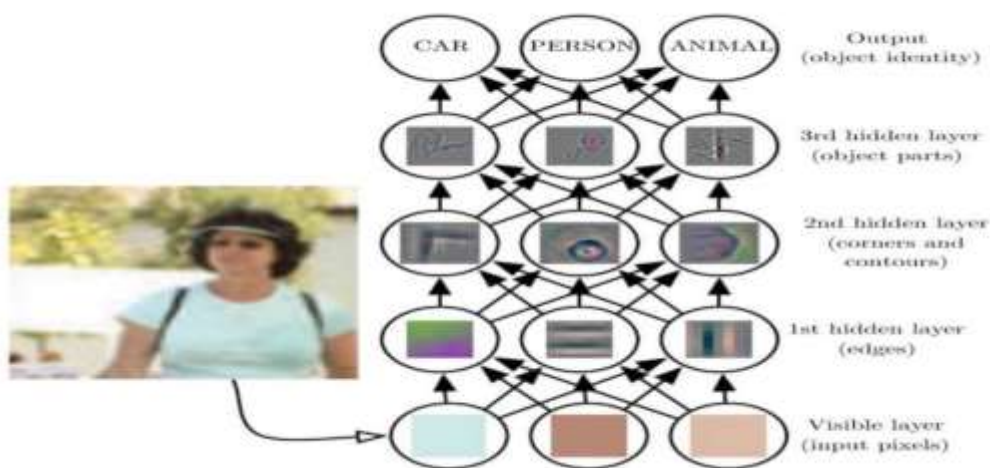


Figure (2.7): Abstract of Deep Neural Network diagram [47].

2.6.1 Deep Neural Networks (DNN)

Hypothetically, deep neural networks (DNN) are artificial neural networks (ANN) with many secret layers. MLP is perhaps the most regularly utilized ANN structure for DNN. Since the neuro network comprises layers of interconnected neurons, it is practically difficult to effectively prepare over a couple of covered-up layers. Given the number of loads in the network that can undoubtedly arrive at thousands or even millions, DNN requires exceptionally huge analytics and taking care of information for preparing stages [53].

2.6.2 Convolution Neural Networks (CNN)

The convolution neural network is one of the most widely used networks in the problem of computer vision, a category of Deep Neural Networks that rely on multi-layered perception (MLP) and techniques backward propagation[54]. They differ from the traditional MLPsr by combining several locally connected layers used for extraction features, followed by several fully connected layers used for classification [55].

The most important characteristic of the NN is local communication and the use of common weights, so that they can identify features local of the portray [26].

Some convolution neural network model consists of three different layers:

- Convolution layers.
- Pooling (or subsamples) layers.
- Fully connected layer (FC).

2.6.2.1 Convolution Layers

When you enter the inputs to this layer, it convolutes it with a constant kernel K to produce n of the feature map, as shown in equation (2.6)

$$Y^l = K^l \otimes X^{l-1} \quad (2.6)$$

K^l Refers to the kernel in the convolution layer, \otimes referring to the operation of convolution. Figure (2.8) shows one kernel convolution with one feature map as output. The output of this layer is mostly through patch normalization to speed the training process and through ReLU non-line activation function as in equation (2.3) [44] [56].

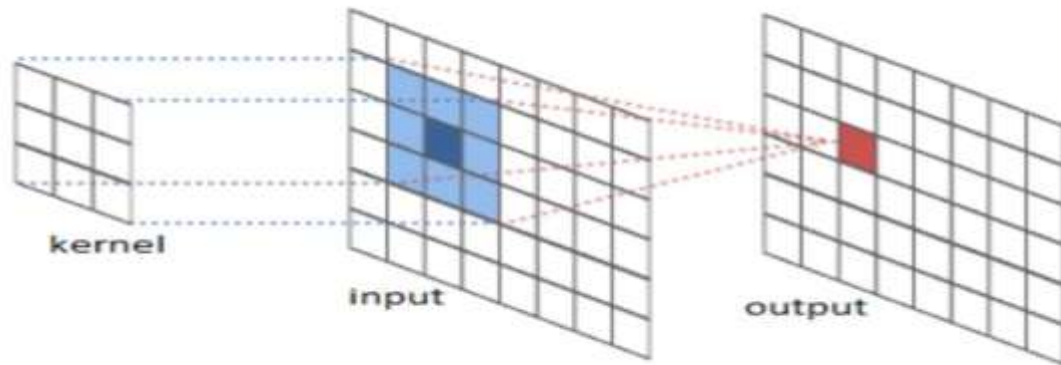


Figure (2.8): Example of convolution layer

2.6.2.2 Batch Normalization

This layer is used to speed up the training process and eliminate sensitivity to network development. It reduces a large number of each channel. First, the activation of each channel is normalized by introducing the mean mini-batch and dividing the standard deviation of the mini-batch. Batch Normalization of its entrance x_i is calculated by mean $\mu\beta$ and variation $\sigma^2\beta$ through a mini-batch and across each input channel as shown in the equation (2.7).

$$\hat{x}_i = \frac{x_i - \mu\beta}{\sqrt{\sigma^2\beta + \epsilon}} \quad (2.7)$$

Here, ϵ (epsilon properties) improves numerical stability when the small difference between the mini Batch variance is very small. To take into consideration the likelihood that the contributions with zero mean contrast and solidarity are not ideal for the layer that follows the batch normalization layer as shown in the equation (2.8).

$$y_i = \gamma \hat{x}_i + \beta \quad (2.8)$$

Here, the scale factor γ and offset β are parameters learnable to update during the training of the network [57] [58].

2.6.2.3 Pooling Layers

Its main objective is to limit. The spatial size of the features maps of the production of the filtering layers, which used almost by the stride $s \in N \geq 2$, which is used to reduce the data to $\frac{1}{s^2}$ of data. Figure (2.9) shows the average pooling how it works.

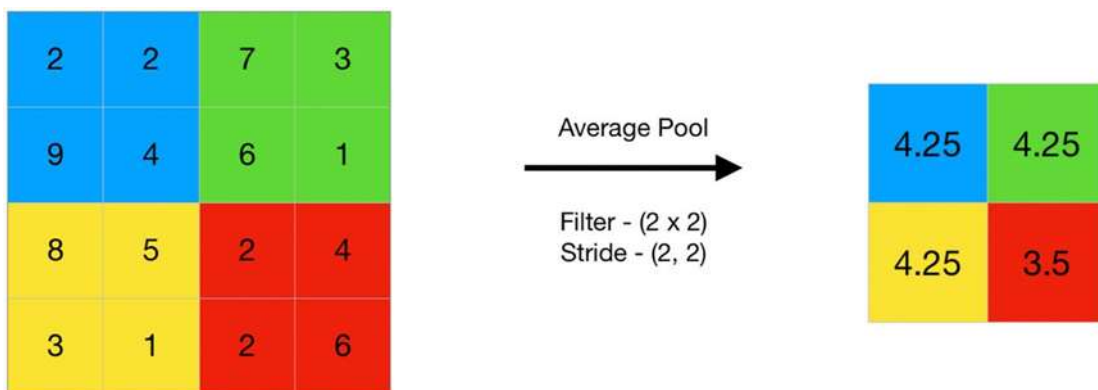


Figure (2.9): Example of average pooling

2.6.2.4 Fully Connected Layers

The fully connected layer is the traditional layer of MLP described where all neural cells in the class are connected to all neural cells in the next class, which is fully related to being used for classification. The dropout technique can be applied to this layer to prevent the problem of over-fitting [56].

2.7 Image Processing Techniques

Biometric information in the images taken requires some preprocessing steps, reduction of noise using the appropriate filtering process, conversion of the filtered image into another (grayscale) image model, and brightness enhancement. Considering that the preprocessing image provides a great deal of vital information such as the pattern of the vein, principle lines, permanent emotions or forms, and the characteristics of the texture, the image is ready to derive the features.

2.7.1 Smoothing Spatial Filter

Smoothing filters are used to blur and reduce noise. Blurring is used in preprocessing steps, such as removing small details from the image before a large organism is extracted and filling small gaps in lines or curves. The use of linear spatial filtering or nonlinear spatial filtering can reduce the noise.

2.7.1.1 Smoothing Liner Filter

The output of a homogeneous linear spatial filter is simply the average of the pixel units near the filter mask. The filtering is sometimes called an average filter. The idea behind the bolstering of the filter is clear and straightforward. By replacing the value of each with the average gray levels in the specified neighborhood by the filter mask, this process produces an image of low transition sharp at gray levels. Considering that random noise usually consists of transition sharp at grey levels, the most obvious application of smoothing is noise reduction.

2.7.1.2 Smoothing Nonlinear

A non-linear spatial filter whose response depends on the pixel units located in the image location of the filter, and then replace the value of the central pixel at the value determined by the result of the arrangement. The most famous example of this type is the median filter.

2.7.1.2.1 Median Filter

The median filter is a technique for processing non-linear that relies on statistics. The loud value of the digital image or sequence is replaced by the median value of the mask. Mask pixel units are arranged to order their grey levels, and the group's median value is stored to replace the loud value. The median filter output is

$$g(x, y) = \text{median} \{f(x - i, y - j, i, j \in w)\} \quad (2.9)$$

Where $f(x, y)$, $g(x, y)$ is the original image and the resulting picture, respectively, W is the mask of two dimensions: the size of the mask is

$(n \times n)$ where n is usually individual such as 3×3 , 5×5 . Maybe the mask form is liner, circular, cross, square, etc.

The median filter has a good ability to preserve the edge and does not offer new pixel values for the treated image.

Median filters are highly popular because, for certain types of random noise, they offer excellent possibilities for reducing noise, with much less distortion than linear filters of similar size. The median filter is particularly effective in the presence of the noise of the impulse. It is

also called salt and pepper noise because of its appearance as white points and black in the image.

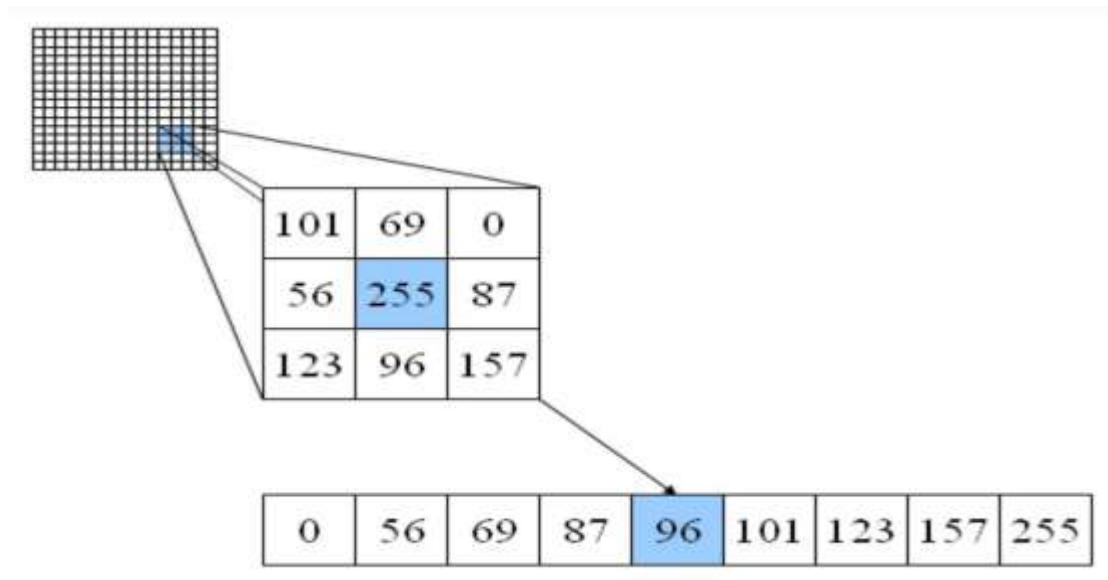


Figure (2.10): Example of median filter

2.7.1.2.2 Anisotropic Diffusion Filter

The primary target of diffusion calculations in picture handling is to eliminate commotion through a fractional differential condition (PDE). In the methodology presented [59], an anisotropic coefficient is utilized to "stop" the dispersion over the edges of the image.

$$\begin{cases} \frac{\partial I}{\partial t} = \text{div}[c(|\nabla I|) \cdot \nabla I] \\ I(t = 0) = I_0 \end{cases} \quad (2.10)$$

Where ∇ is the gradient operator, div the divergence operator, $|\nabla I|$ denotes the magnitude, $c(x)$ the diffusion coefficient, and I_0 the initial image. They suggested two diffusion coefficients

$$C(x) = \frac{1}{1 + (x / 2)^2} \quad (2.11)$$

And

$$C(x) = \exp[-(x/k)^2] \quad (2.12)$$

Where k is an edge magnitude parameter in the anisotropic diffusion method, the gradient magnitude is used to detect an image edge or boundary as a step discontinuity in intensity [56]. If $|\nabla I| > k$, $c(|\nabla I|) \rightarrow 0$, and have an all-pass filter $|\nabla I| < k$, $c(|\nabla I|) \rightarrow 1$, and achieve isotropic diffusion (Gaussian filtering).

$$I_s^{t+\Delta t} = I_s^t + \frac{\Delta t}{|n_s|} \sum_{p \in n_s} c(|\nabla I_{s,p}^t|) \nabla I_{s,p}^t \quad (2.13)$$

Where I_s^t is the discretely sampled image, s denotes the pixel position in a discrete two-dimensional (2-D) grid, and Δt the time step size, n_s represents the spatial neighborhood of a pixel $|n_s|$ is the number of pixels in the window (usually four, except at the image boundaries) [56], and

$$\nabla I_{s,p}^t = I_p^t - I_s^t, \forall p \in n_s \quad (2.14)$$

The advantages of anisotropic diffusion include intra-region smoothing and edge preservation. Anisotropic diffusion performs well for images corrupted by additive noise. Several enhancements and edge detection methods have been described in the literature for images with additive noise. In cases where images contain speckle, anisotropic diffusion will enhance the speckle, instead of eliminating the corruption [56].

2.7.2 Image Segmentation

Segmentation refers to the process of dividing the image into constituent parts or to separate organisms. Segmentation aims to simplify and/or change the representation of the image to something more important and easier to analyze [60].

The division is usually used to determine the location of organisms and boundaries (line and curves) in the images. In more precise terms, the splitting of the image is the process of designating each by the seal in the image so that the pixel units with a similar name share certain visual qualities. The consequence of the Division of the picture is a bunch of fragments that cover the entire picture or a bunch of highlights separated from the picture. Every investigation in an area is comparable to a specific or determined trademark, like tone, thickness, or surface [10].

The division is the most important part of image processing. Conversion of the whole image into several parts, which is more important and easier to address further. It will cover the many parts that have been included in the whole image. The division may also depend on many of the features contained in the image. It may be a color or a fabric. The division is also useful in analyzing images and pressuring

images. In the following subsections, a brief explanation of the famous image Segmentation technology [10].

The threshold is a vital part of the image segmentation, where objects are isolated from the background. It is the simplest way to split the picture. This method relies on the level of cap-off (or value threshold) to convert a grayscale image into an image binary. The key to this method is to determine the value of the threshold (or values at multiple levels) [10].

The distribution of objects density and background pixel is sufficiently distinct, so threshold General (individual) can be used in the entire image.

When threshold depends only on the gray level of the picture and threshold is the only link to the characteristics of the pixel in the images, this technique is called the global threshold [61]. It consists of the determination of the fixed threshold, and all pixel values below the threshold refer to the background and those above the fixed value are considered in the foreground.

$$g(x, y) = \begin{cases} 1, & \text{if } f > Thr \\ 0, & \text{if } f \leq Thr \end{cases} \quad otherwise \quad (2.15)$$

Where $g(x, y)$ is the output image after the threshold. Examples of the global threshold are the Otsu threshold [10].

In computer vision and image processing, the Otsu method, named Nobuyuki Otsu, is used to perform the automatic threshold of images. In its simplest form, the algorithm returns a single severity limit that separates pixel units into two categories, foreground, and background. This threshold shall be determined by reducing the intensity variation

within the category, or in an equivalent manner, by maximizing the disparity between categories. The Otsu method is a separate, one-dimensional analog for the analysis of the special fiction, and equates to the global optimum method performed on the density chart. Figure (2.11) shows the Otsu method.

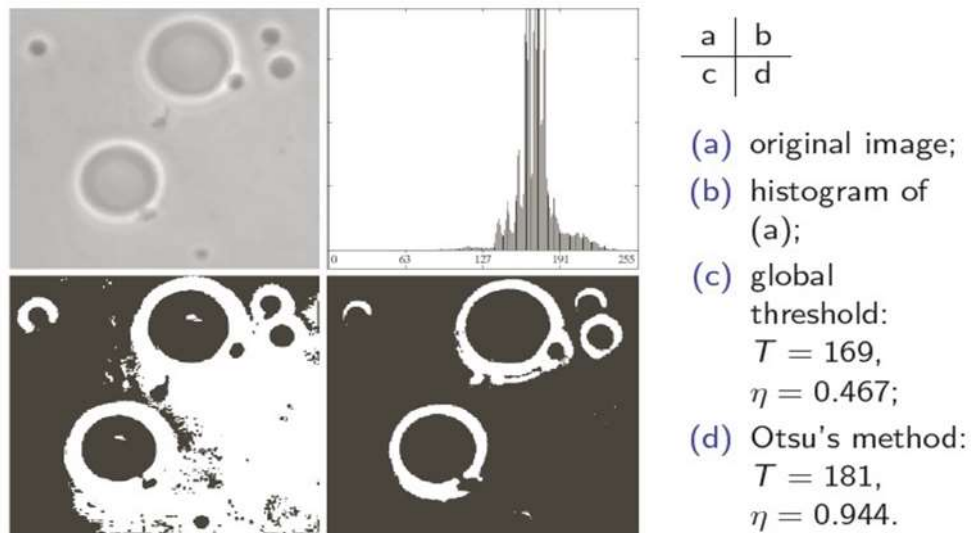


Figure (2.11): Otsu method [10]

2.7.3 Morphology Operation

Morphology is a section of image processing and is particularly useful for the analysis of the forms in the images. Basic morphological tools are applied to examine bilateral images, and then clarify how these tools can be expanded to include greyscale images. Morphological methods include filtering and thinning. All morphological functions are identified for the binary image, but most of them have a natural extension of grey images. Erosion and Dilation are the basic processes of morphology, meaning that all other processes are based on a combination of these processes [60]. It is defined in terms of the initial group operations but used as an essential element of many algorithms.

Both erosion and dilation are produced through the interaction of a group called structural elements with a set of pixel units that concern the image. The structure element has form and origin[8]. Operations are:

2.7.3.1 Dilation

Dilation (usually represented by \oplus) is one of the key processes in segmentation processes. Originally developed for binary image, it was expanded first to graphic images, and then to complete the snap. The expansion process usually uses a structural component to examine and expand the formats in the form of an introduction.

A is a set of pixels and B is a structural element. (B^s) is a reflection of B around its origin and follows a displacement by s. Dilation as shown in figure (2.12), is expressed as $A \oplus B$ are the set of all transformations that achieve:

$$A \oplus B = \{s | (B^s) \cap A\} \quad (2.16)$$



Figure (2.12): Dilation process [8]

The equation (2.16) depends on the reflection of B about its origin and the conversion of this reflection for s. A and B is a set of all the displacement. As in the past, it is assumed that B is a structural element

and that A is the group to be expanded or could say that B fluctuates around its origin and slip above group A. Expansion is used to repair breaks [8].

2.7.3.2 Erosion

The Erosion (usually represented by \ominus) is one of two segmentation processes (the other is dilation) in the processing of morphological images on which all other morphological processes are based. Originally defined for binary images, it was later extended to graphic images. The erosion process usually uses a structural element to examine and reduce existing forms of input.

A is a set of pixels and B is a structural element shown in figure (2.13) and the equation of it is

$$A \ominus B = \{s | (B) s \leq A\} \quad (2.17)$$

Erosion can lead to the division of related organisms and can eliminate the emission. Erosion of deflation or mitigation is used while dilation grows and organisms are stunned in the binary image [68]. If the image continues to erosion, it will end with a completely black result [60]. Figure (2.13) shows the erosion process.



Figure (2.13): Erosion process [8]

2.7.3.3 Opening

The Erosion (usually represented by \ominus) in the morphology operation, the opening operation is dilation of the erosion of a set of A by structural element B

$$A \circ B (A \ominus B) \oplus B \quad (2.18)$$

The opening leads to the removal of small organisms from the front of the image (usually captured as units with bright) of the image, placing them in the background [10].

2.7.3.4 Closing

The closing (usually represented by \cdot) in the morphology operation, the closing operation is the erosion of the dilation of a set of A by structural element B

$$A \cdot B (A \oplus B) \ominus B \quad (2.19)$$

The closing operation removes the small closures at the front, and the small holes change the background to the forefront. These methods can also use to find certain forms in some form [10].

2.7.3.5 Boundary Extraction

The boundary of group A referred to as $B(A)$, can be obtained by erosion first A from B and then make the specific difference between A and their erosion. This is

$$B(A) = A - (A \ominus B) \quad (2.20)$$

Where B is an appropriate structural element. Figure (2.14) clarifies the mechanisms for extracting the border. It shows a simple

binary object, B component, and the result of using the equation (2.17). Figure (2.14) shows the boundary extraction [10].

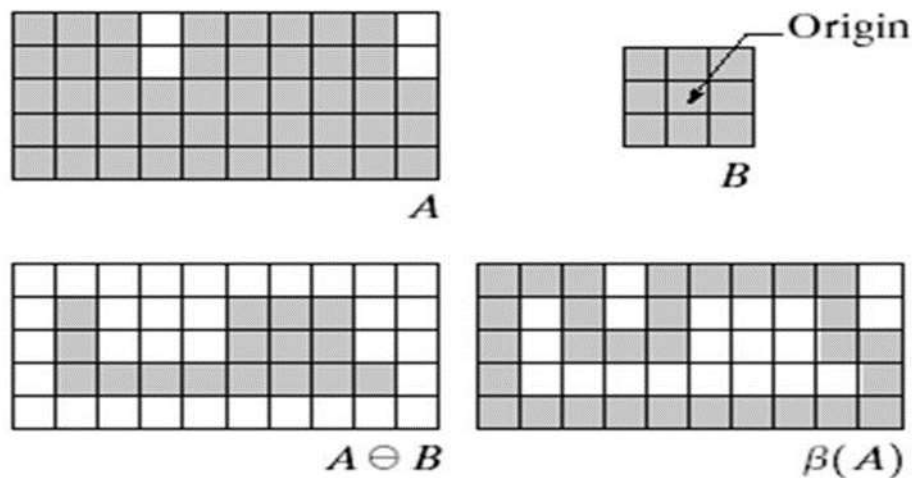


Figure (2.14): Boundary extraction [10]

2.8 Performance Measures

In our work, extracted the accuracy for each band and each of the three cases implemented in the training and testing phase, for both the right and left hands. Then applied a confusion matrix and extracted values from it Sensitivity, Specificity, Precision, and F-Score.

2.8.1 Confusion Matrix

A confusion matrix is a method for summing up the presentation of an arrangement calculation. Classification accuracy alone can be deceiving if you have an inconsistent number of perceptions in each class or on the other hand on the off chance that you have multiple classes in your dataset. Computing a confusion matrix can give you a superior thought of what your arrangement model is getting right and what types of errors it is making.

2.8.2 Sensitivity (Se):

The ability of the test to effectively identify people through the veins.

$$Se = \frac{TP}{TP + FN} \quad (2.21)$$

2.8.3 Specificity (Sp):

The ability of the test to accurately distinguish individuals who are not registered in the database through the veins.

$$Sp = \frac{TN}{TN + FP} \quad (2.22)$$

2.8.4 Precision (Pr):

Allowed to the measure of data that is passed on by a number as far as its digits; it shows the closeness of at least two estimations to one another. It is autonomous of accuracy.

$$Pr = \frac{TP}{TP + FP} \quad (2.23)$$

F-Score (F):

F-measure or F-score measures the accuracy testing.

$$F = \frac{2 * TP}{2 * TP + FP + FN} \quad (2.24)$$

Chapter 3 - Design principles and preparation

Chapter Three

Design principles and preparation

3.1 Introduction

In this chapter, the design and implementation of the identification of the proposed palm vein will be present. It contains all details of each stage and process of the system in place.

3.2 Proposed System

Our proposed system goes through two basic stages: the first stage is the preprocessing stage to extract the region of interest and remove the noise in the images and the second stage is the proposed convolution neural network (CNN) stage to extract the features, classify the image and identify for any person affiliated.

The palm vein based identification system based on the deep learning method consists of two main phases: Registration phase (or system training phase) including preprocessing training data and templet storage. The subsequent identification phase (system test phase) consists of preprocessing testing data, matching and decision. The proposed chart of the system is shows in figure (3.1) and explains how the system operates. Each one will discuss in detail. Figure (3.1) shows the diagram of the proposal system.

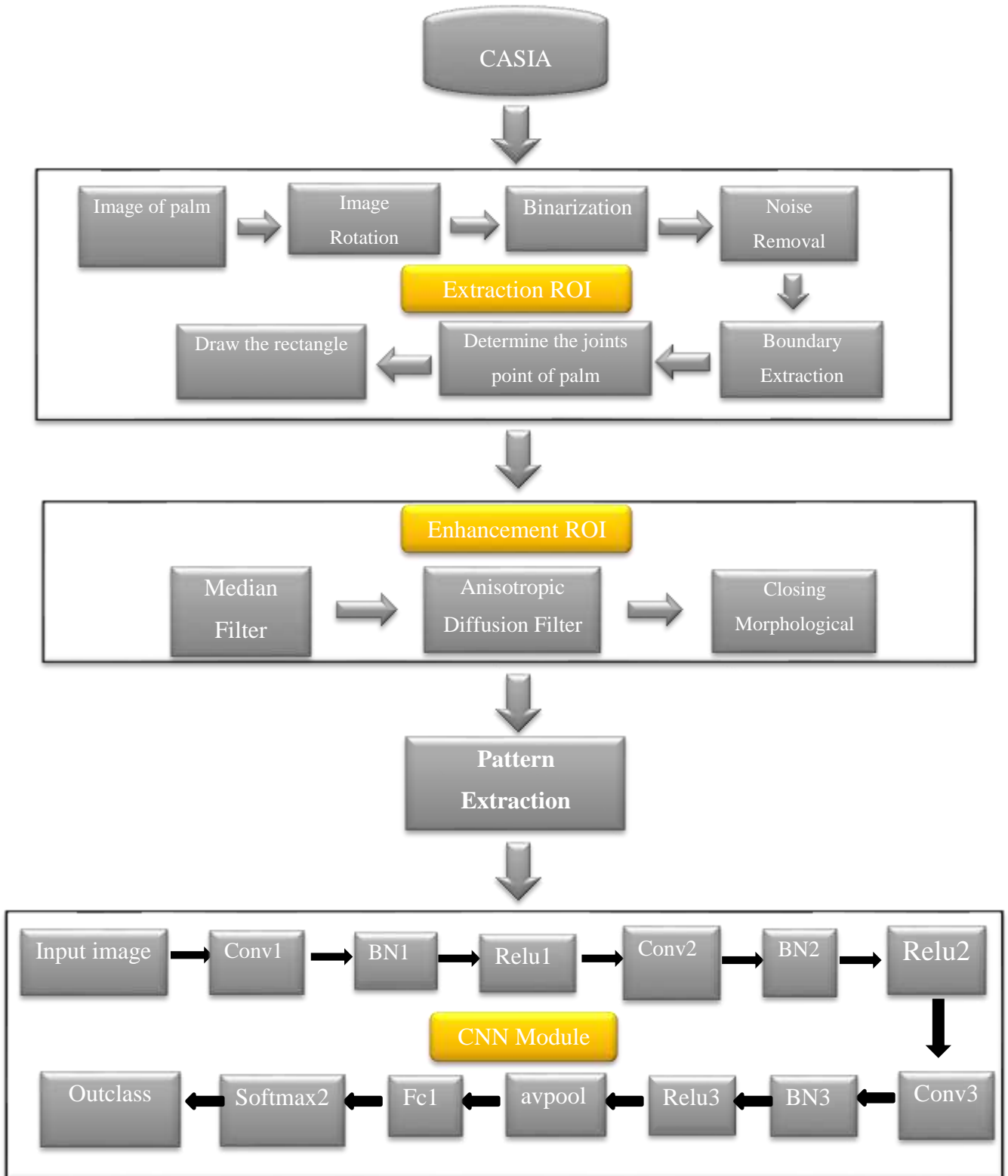


Figure (3.1): The diagram of proposal system

3.3 Image Preprocessing

Preprocessing of the image is the first stage that applies to the improvement of palm print images. The aim is to show the details of the image well, because sometimes the images may take in unfavorable light and noise conditions, and this process is completed simultaneously.

3.3.1 Preprocessing Stage for Palm Vein

The preprocessing phase is important to simplify the task of insulation of the palm from the background. Despite many devices used to capture the palm, some images are bad, some good, or some take all palm with their perimeter and the fingers and loud backgrounds. To ensure the performance of the algorithms used to extract features and isolate the vein from the palm, a range of processes must be applied to improve and address these cases from the introduction image. A range of improvement tasks has been implemented to improve the clarity of the structure of the vein pattern and to determine the region of interest (ROI) of the veins. The preprocessing phase of the image shall be the basic stage of the biometric system. Some parts of the veins will be invisible in some images. The aim of preprocessing is to improve some of the important features of the image of features processing or to improve image data containing undesirable distortions.

3.3.2 Palm Vein Region of Interest (ROI)

The purpose of the extraction of the region of interest (ROI) is to remove image regions that do not contribute to the beneficial advantages of characterizing or classifying images. It tries to redefine

the borders within the image obtained. This smaller region is the focus region for the application of different deriving and classification strategies. The region of interest is expected to improve the accuracy of identification and validation. An important step is to extract the features region of interest, which is important for the performance of identification to develop the accuracy of the definition.

The region of interest is a region rich in features and it is important to perform recognition of the development of the accuracy of identification. The region of interest for palm vein must be very effective. There are five substrates to obtain a return on investment:

3.3.2.1 Image Rotation

The image in the database that used in our thesis is taken in several directions and with different movements because no rest supports the hand until it is captured with a good picture of the hand. rotated the images until they were all equal in direction to make it easier for us to extract the important region of the veins Figure (3.2) shows us the rotation method.

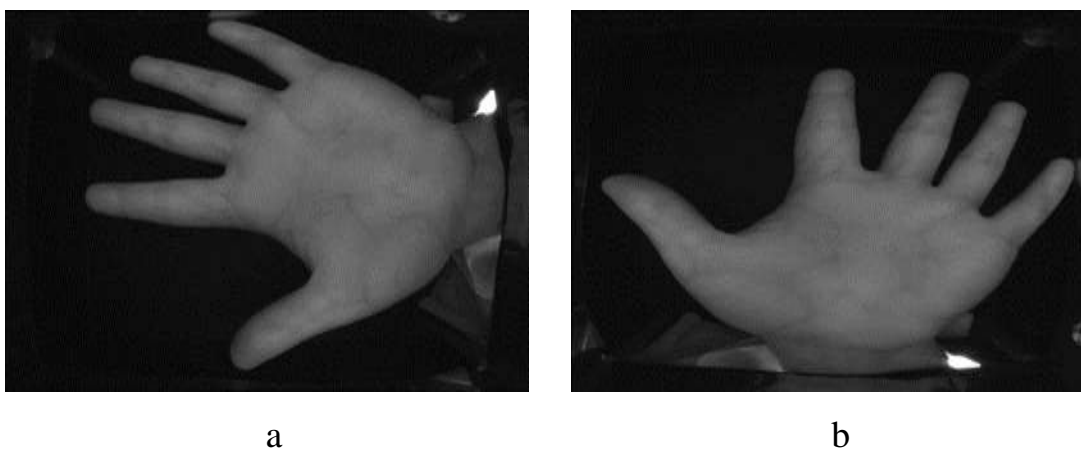


Figure (3.2): Rotation method (a) The original image (b) Image after rotate

3.3.2.2 Binarization

In this step, after rotating the image, the gray image is converted into a binary image using the Otsu method, which is one of the most important conversion methods and is considered a global threshold. figure (3.3) shows us the result of this method after applying it to the image of the palm.

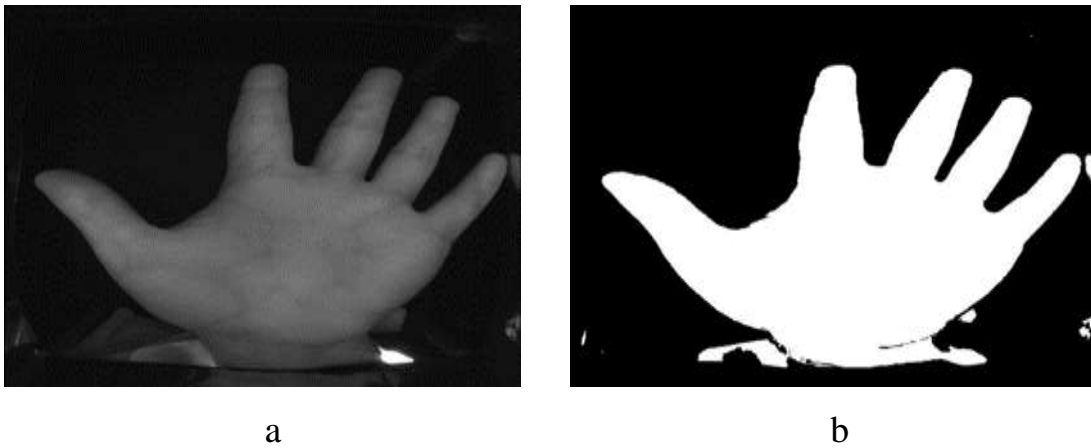


Figure (3.3): Otsu method (a) The rotate image (b) Image after Otsu threshold

Algorithm 3.1 Otsu threshold**Input:** rot_image**Output:** bin_image**Goal:** binary image1: **procedure**

2: Compute the histogram and probabilities of each intensity level

3: $\omega \leftarrow 0$ 4: $\mu \leftarrow 0$ 5: compute $\sigma_b^2(t)$ 6: Step through all possible thresholds $t=1, \dots$

7: Maximum intensity

8: update ω_i, μ_i 9: compute $\sigma_b^2(t)$ 10: **return** The desired threshold corresponds to the maximum $\sigma_b^2(t)$ 11: **end procedure***Algorithm 3-1 Otsu threshold***3.3.2.3 Noise-Removal**

The input image has been fully captured with some unwanted things, which need to be discarded before moving on to the next stage. At this stage, after converting the image into image binary, it is easy to extract the ROI. Some unwanted parts appeared on the side of the palm, so implemented an opening morphological process to remove these unwanted parts. The best arrangement statistics and the nonlinear spatial filter is the median filter. Have also applied some processes to remove the noise after extracting the ROI, and these processes are the median filter that leads to a better result using equation (2.9).and the other filter is an anisotropic diffusion filter. In this thesis, use the median filter, anisotropic diffusion filter, closing opening operation, and closing

operation for removing noise after identifying the critical points in the palm and extracting the ROI figure (3.4) shows us the opening operation.

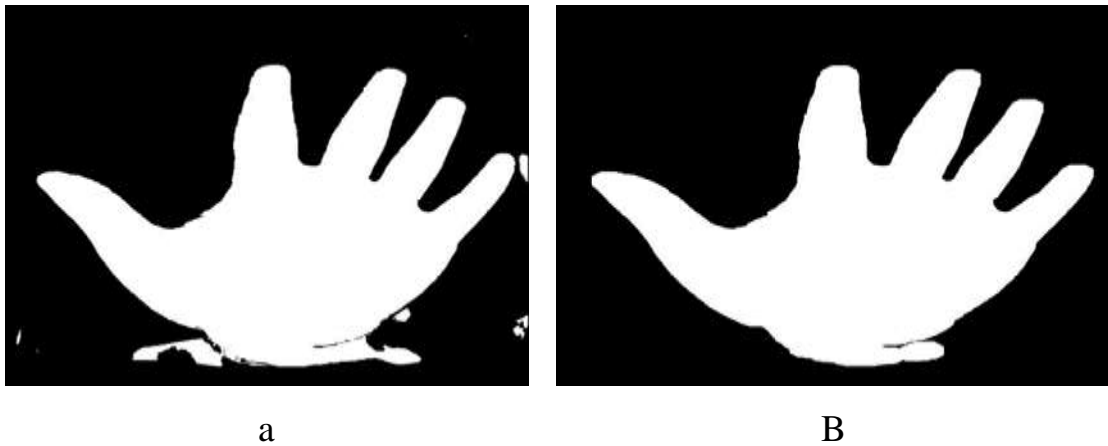


Figure (3.4): Opening operation (a) image after Otsu threshold (b) Noise Removal after opening morphological operation

3.3.2.4 Boundary Extraction

The boundary of the palm region is required for the next steps to determine the benchmarks that have derived the region of interest. Application of border extraction using the extraction of a morphological boundary in the equation (2.20). Figure (3.5) shows the extraction boundary.

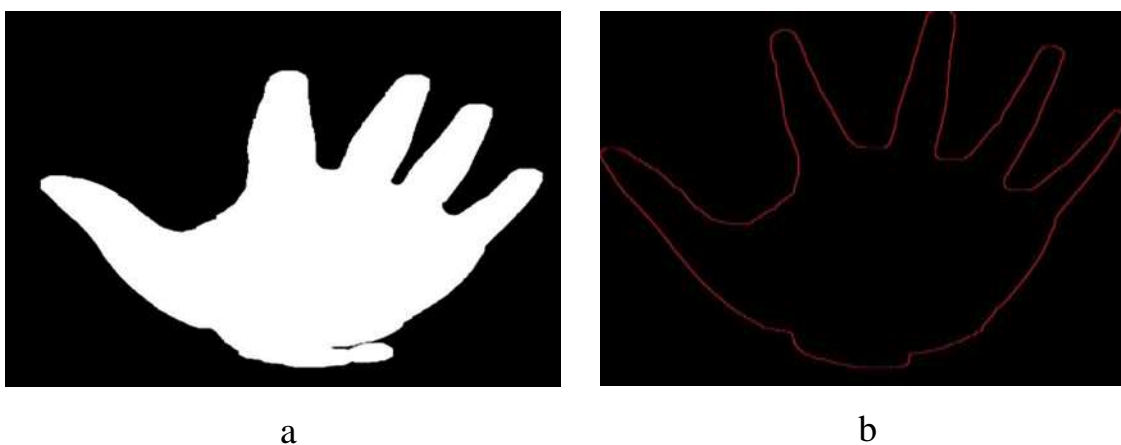


Figure (3.5): Extraction boundary (a) Noise Removal after opening morphological operation (b) Boundary extraction

3.3.2.5 Determination of the joint points of the palm

1. Determine joints by scanning a vertical one image after another until up to nine (or more) with vertical sequences, when these pixels are obtained, a green circle must be put in this place and one of the other points should be considered in the same way as illustrated in figure (3.6).
2. Select the area of the gathering to the thumb, then, at that point start the other way and set the primary level as the main point (p1) delineated in Figure (3.6).
3. The reference focuses to use for the locale of interest are the principal point between the little and ring fingers, for example, (p1), and the subsequent point is the point between the center finger and the forefinger (p3). These focuses are viewed as joint focuses.
4. Point second was distinguished through the joint third and a straight line was drawn between two-point (P1, P3).
5. Of these points, draw the region of interest (ROI).

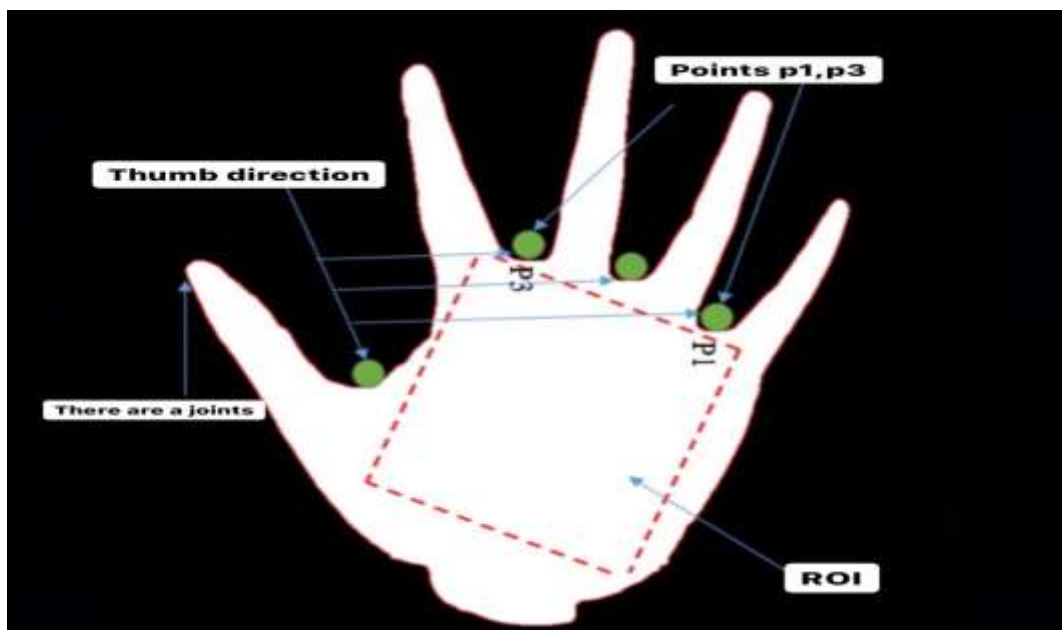


Figure (3.6): The diagram of the important point in the palm

Algorithm 3.2 Extraction ROI

Input: Boundary extraction W, H
Output: ROI
Goal: extract the region of interest

```

1: procedure
2:   Step1: Determine thumb direction
3:    $c \leftarrow 0$ 
4:   for  $i \leftarrow 0$  to  $W$  do
5:     for  $j \leftarrow 0$  to  $H$  do
6:       if  $(\text{Img}[i, j] = \text{green})$  and  $(i = \text{point})$  then
7:          $\text{point} = i$ 
8:       end if
9:     end for
10:  end for
11:  Step2: Determine reference points
12:  for  $i \leftarrow 0$  to  $\text{point} - 1$  do
13:    for  $j \leftarrow 0$  to  $W$  do
14:      if  $(\text{Img}[i, j] = \text{green})$  and  $(c = 0)$  then
15:         $p1x = i$ 
16:         $p1y = j$ 
17:        increment
18:      else if  $(\text{Img}[i, j] = \text{green})$  and  $(c = 1)$  then
19:         $p1x = i$ 
20:         $p1y = j$ 
21:        increment
22:      else if  $(\text{Img}[i, j] = \text{green})$  and  $(c = 2)$  then
23:         $p2x = i$ 
24:         $p2y = j$ 
25:        increment
26:      else if  $(\text{Img}[i, j] = \text{green})$  and  $(c = 3)$  then
27:         $p3x = i$ 
28:         $p3y = j$ 
29:        increment
30:      end if
31:    end for
32:  end for
33:  Step 3: draw line between two reference points
34:  draw line  $(p1, p3)$ 
35:  Step4: draw rectangle (ROI)
36:   $H \leftarrow \text{line-Distance}(\text{green\_point}, \text{End\_line})/2$ 
37:   $W \leftarrow H$ 
38:  return draw rectangle  $(p1, p3, W, H)$ 
39: end procedure

```

Algorithm 3-2 Extraction ROI

3.3.3 Enhancement image of the region of interest

Image improvement is the way toward altering advanced images with the goal that the outcomes are more inventory cordial or more image examination. For instance, you can eliminate the noise or make the image more intense or accessible, making it simpler to recognize the essential highlights.

3.3.3.1 Median filter

The median channel is one of the mainstream measurable channels because of the great exhibition of some particular commotion types, for example, "Gaussian", "random", and "salt and pepper". As indicated by the transitional channel, the mean pixel in the $m \times m$ region replaces the middle worth of the comparing window. Note that the commotion pixel is different from the normal.

Utilize this channel to eliminate pixel clamor on palm vein picture after removing the district important to work with separate example vein. Figure (3.7) shows the median filter.

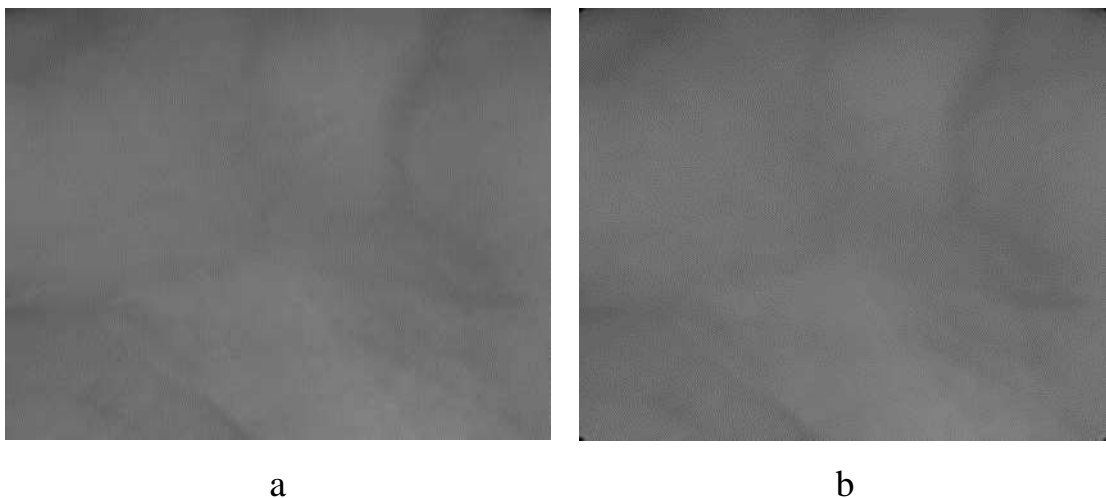


Figure (3.7): Median filter (a) The region of interest (b) The ROI after median filter

3.3.3.2 Anisotropic diffusion filter

It is a way to improve the quality of the image of organisms while preserving the edge of the object. It removes the effects of confusion while reducing disguise and maintaining details in sub-regions.

The filter was selected because it keeps the edges while the noise was removed. In general, differing characteristics are used in the algorithms of edge detection. Such algorithms are working on a brink that seeks diffusion coefficient factor that breaks the multifaceted image. Each fixed multiple-defined image has limits among the persistent ingredients that detected edges. Figure (3.8) shows the anisotropic filter.

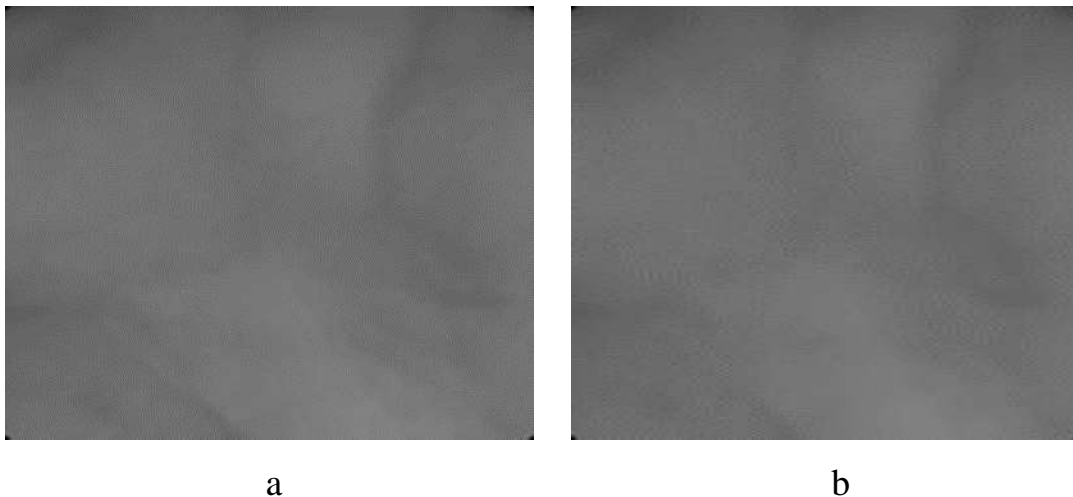


Figure (3.8): Anisotropic filter (a) The ROI after the median filter (b) The ROI after Anisotropic diffusion filter

3.3.3.3 Closing Morphological Operation

Closing is an important factor in the field of morphological mathematical science. Like the opening of the dual operator, it can be derived

from basic dilation and erosion processes. Such operators are usually applied to image binary, despite the existence of gray-level releases. Closing in some respects is similar to extension in that it tends to expand the border of the front areas in the image (to reduce the background color holes in such areas), But the least destruction of the underlying form of borders, as in other morphological factors, is controlled by a structural element. The functional factor impact to preserve the background is similar to the structural element. Figure (3.9) shows the Closing operation.

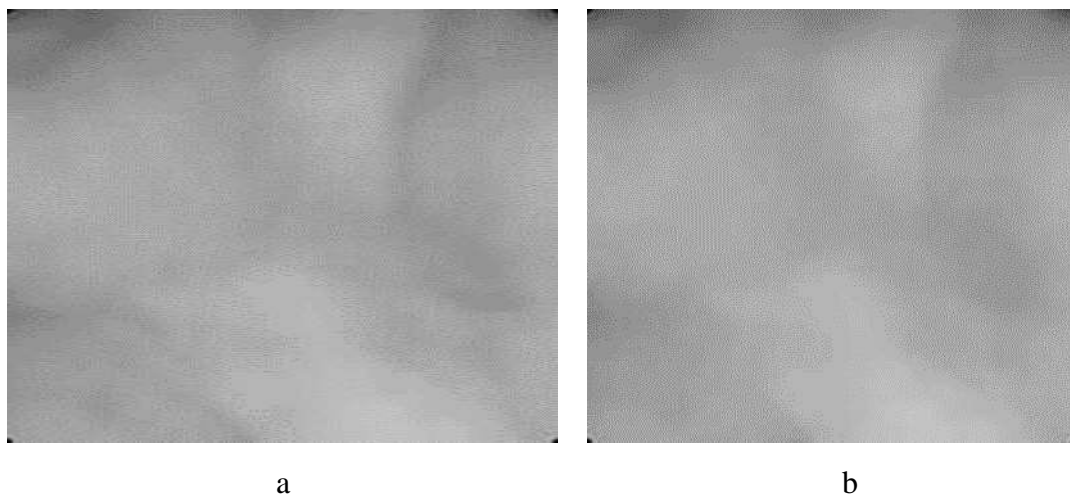


Figure (3.9): Closing operation (a) The ROI after Anisotropic diffusion filter (b) The ROI after closing morphological operation

3.4 Pattern Extraction

After applying the median filter, anisotropic diffusion filter, and closing morphological operation subtract one image from another, subtract constant from image and Adjust image intensity values, or color map. To get a clear vein pattern until entering it in the proposed

convolution neural network. Figure (3.10) shows the extraction pattern of the vein.

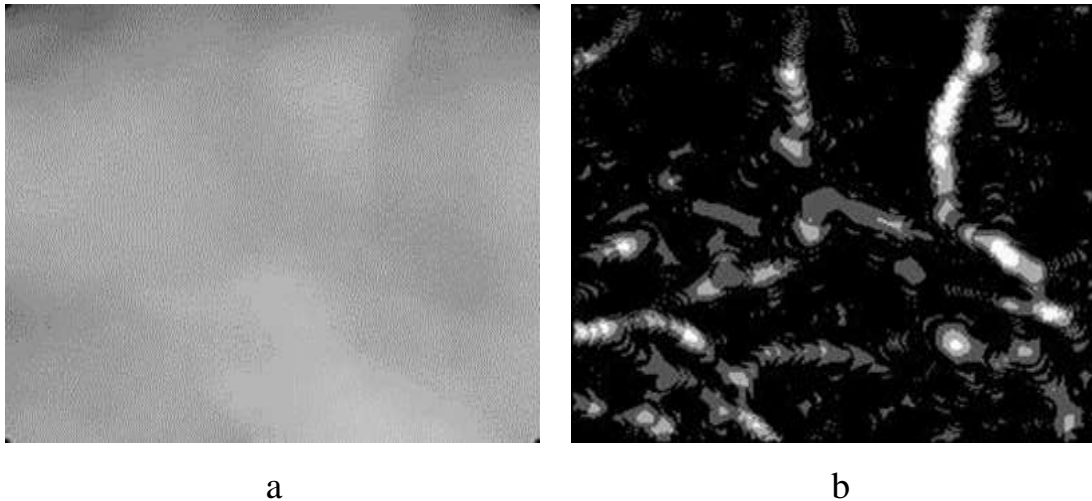


Figure (3.10): Extraction pattern (a) The ROI after closing morphological operation (b) Extraction pattern of vein

3.5 Feature Extraction

The most important stage in the identification system is profiling feature extraction such as the edge of the line, angles, statistical features, and more in the main proposal. The system uses the nervous neural network (CNN), a convolution layer that plays the role of the extraction phase. Figure (3.11) indicates the layers of CNN used. Each layer will then explain in detail:

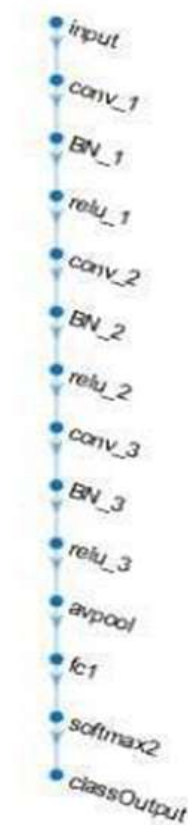


Figure (3.11): The layer of proposed Convolution Neural Network

3.5.1 Palm Vein Identification System Based on proposed CNN

The Convolutional Neural Network (CNN) used in this thesis consists of these layers. The first is an image input layer, which takes as input a resized grayscale image of 32 by 32 dimensional. On top of the input, it has three convolutional layers, every one of which is trailed by a batch normalization layer and a ReLU layer. The three convolutional layers use channels of size 23. It has an alternate number of channels, separately 16, 64, and 32. Convolution layers are trailed by an Average pooling layer, the width and the step of the normal pooling layers are both double cross advances. The convolutional layers are stacked with

a fully connected layer. This layer is comprised of 100 units. The Softmax activation layer and a classification layer follow this layer. This network is similar to many networks proposed to deal with the problem of palm digit writing, this is due to the similarity of the patterns in the images of palm write digits and the images of the palm veins. table (3.1) shows the details of these layers.

Using Convolutional neural networks CNN in which the network is based on convolution layers; in our experiment, have baser our architecture on three convolutions, each convolution is successes by a batch Nrml layers and a ReLU activation layers (as all recommendations on CNN implementation). So have nine layers (conv1 + batch Nrml + ReLU) * three and it has the input and output layers those are 11 layers the remaining three layers are the average pooling layer + two layers which are (softmax layer and classification layer). Figure (3.12) shows the proposed CNN Architecture for palm vein recognition.

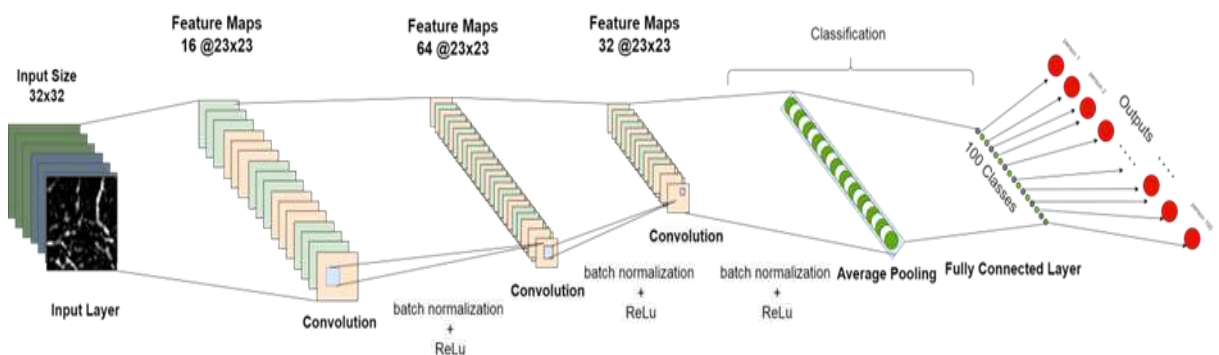


Figure (3.12): Proposed CNN Architecture for palm vein recognition

Table 3-1 the details of these layers

	Name	Type	Activation	Learnable
1	Input	Image input	32*32*1	-
2	Conv_1	Convolution	32*32*16	Weight 23*23*1*16 Bias 1*1*16
3	BN_1	Batch normalization	32*32*16	Offset 1*1*16 Scale 1*1*16
4	Relu_1	ReLU	32*32*16	
5	Conv_2	Convolution	16*16*64	Weight 23*23*16*64 Bias 1*1*64
6	BN_2	Batch normalization	16*16*64	Offset 1*1*64 Scale 1*1*64
7	Relu_2	ReLU	16*16*64	
8	Conv_3	Convolution	16*16*32	Weight 23*23*64*32 Bias 1*1*32
9	BN_3	Batch normalization	16*16*32	Offset 1*1*32 Scale 1*1*32
10	Relu_3	ReLU	16*16*32	
11	Avpool	Average pooling	8*8*32	
12	Fc	Fully connected	1*1*100	Weight 100*2048 Bias 1*100
13	Softmax2	Softmax	1*1*100	-
14	Class output	Classification output	-	-

3.5.1.1 Convolution Layer (Conv)

The convolution layers use filters on the inputs that have been entered into this layer to make the filters have a size $f \times f$, where the

filters do the c while scanning the inputs. In addition, use steps that you move over the entries called stride and their dimensions are $s \times s$ to produce what is called activation map or feature map to make the entrance to the next layers, the convolution layer is considered one of the most time-consuming layers.

3.5.1.2 Batch normalization layers (BN)

This layer is used to speed up the training process and eliminate sensitivity to network development, reducing a large number of each channel. First, the initiation of each channel is standardized by deducting the mean of the small cluster and partitioning it by the standard deviation of the smaller than usual clump, after which the layer is dislodged by offset β , and afterward the scale factor γ . This layer is used between the convolution layer and the RLeU layer. Algorithm (3.3) illustrates the algorithm of the batch normalization.

Algorithm 3.3 Batch normalization**Input:** Feature_map**Output:** Nrm1.Feature_map**Goal:** speed up the training process1: **procedure**

2: $\mu_\beta \leftarrow \frac{1}{m} \sum_{i=1}^m x_i$ ▷ mini_batch mean

3: $\sigma^2_\beta \leftarrow \frac{1}{m} \sum_{i=1}^m (x_i - \mu_\beta)^2$ ▷ mini_batch variance

4: $\hat{x}_i \leftarrow \frac{x_i - \mu_\beta}{\sqrt{\sigma^2_\beta + \epsilon}}$ ▷ normalize

5: $y_i \leftarrow \gamma \hat{x}_i + \beta \equiv BN_{\gamma, \beta}(x_i)$ ▷ scale and shift

return y_i 6: **end procedure***Algorithm 3-3 Batch normalization***3.5.1.3 Rectified Liner Activation Function (ReLU)**

Considering that, images are not naturally taken and contain nonlinear features such as color and borders, the function of the rectified linear activation is applied to increase nonlinear image. For example, the RLeU layer is used to ensure a strong feature only by taking positive numbers only and Conversion of all negative numbers to zero as shown in algorithmic (3.4).

Algorithm 3.4 Activation function ReLU

Input: *Nrml_Feature_map*
Output: *Re_Feature_map*
Goal: create nonlinear image (feature map)

```

1: procedure
2:   for  $x \leftarrow 0$  to column do      ▷ Feature map width after max pooling
3:     for  $y \leftarrow 0$  to row do      ▷ Feature map height after max pooling
4:       if  $Feature\_map(x, y) < 0$  then  ▷ if current value is negative
5:          $Re\_f\_map(x, y) \leftarrow 0$     ▷ set current value to zero
6:       else
7:          $Nrml\_Feature\_map(x, y) \leftarrow Re\_map(x, y)$ 
8:       end if
9:     end for
10:  end for
11:  return Re_Feature_map

```

Algorithm 3-4 Activation function ReLU

3.5.1.4 Average Pooling Layer (AP)

To choose the best feature in the image and compare it to other images to identify people, the average is calculated for each patch in the feature map. This means, for each area in the feature map $2 * 2$ square passed over and the average calculated for it, and so on passed across the entire matrix. Algorithm (3.5) illustrates the algorithm of the average pooling.

Algorithm 3.5 Average pooling**Input:** Re_Feature_map (3)**Output:** Ave_Feature_map**Goal:** choice important feature

```

1: procedure
2:   for  $i \leftarrow 0$  to Height:stride do      ▷ stride refer to increment value
3:     for  $j \leftarrow 0$  to width:stride do
4:       for  $x \leftarrow 0$  to  $i + \text{win\_size}$  do  ▷ represent initial mask position
5:         for  $y \leftarrow 0$  to  $j + \text{win\_size}$  do  ▷ win_size=region of the filter
6:            $H \leftarrow$  Average value lies under mask
7:         end for
8:       end for
9:        $\text{Ave\_Feature\_map}(i, j) \leftarrow H$ 
10:    end for
11:  end for
12:  return Ave_Feature_map
12: end procedure

```

*Algorithm 3-5 Average pooling***3.5.1.5 Fully Connected Layer (FC)**

This layer is the place where every one of the contributions from one layer interfaces with every activation unit of the following layer. In most normal AI models, the last layers are completely associated layers that consolidate the information separated by the past layers to shape the last yield. This layer is the subsequent tedious layer after the convolution layer.

3.6 AlexNet

The AlexNet network is a convolutional neural network with great order execution. This network comprises five convolution layers and three completely associated layers. The channel size is between 3×3 to 11×11 and 3 to 256 channels for each channel size. The pooling layer applies max-pooling activity inside 3×3 layers 1, 2, 5. The AlexNet network handles the information pictures of 227×227 and contains 61 million weight. Figure (3.13) shows the Architecture of AlexNet

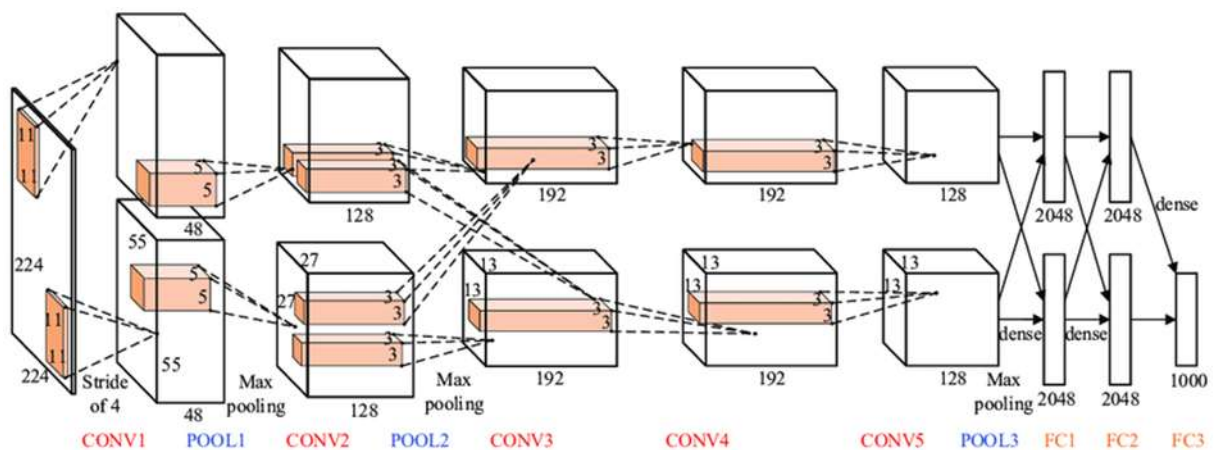


Figure (3.13): The Architecture of AlexNet

Table 3-2 the details of AlexNet layers

	Name	Type	Activation	Learnable
1	data	Image Input	227*227*3	0
2	conv1	Convolution	55*55*96	34944
3	relu1	ReLU	55*55*96	0
4	norm1	Cross Channel Normalization	55*55*96	0
5	pool1	Max Polling	55*55*96	0
6	conv2	Convolution	27*27*256	307456
7	relu2	ReLU	27*27*256	0
8	norm2	Cross Channel Normalization	27*27*256	0
9	pool2	Max Polling	13*13*256	0
10	conv3	Convolution	13*13*384	885120
11	relu3	ReLU	13*13*384	0
12	conv4	Convolution	13*13*384	663936
13	relu4	ReLU	13*13*384	0
14	conv5	Convolution	13*13*256	44262
15	relu5	ReLU	13*13*256	0
16	pool5	Max Polling	6*6*256	0
17	fc6	Fully Connected	1*1*4096	37752832
18	relu6	ReLU	1*1*4096	0
19	drop6	Dropout	1*1*4096	0
20	fc7	Fully Connected	1*1*4096	16781312
21	relu7	ReLU	1*1*4096	0
22	drop7	Dropout	1*1*4096	0
23	fc8	Fully Connected	1*1*1000	4097000
24	prob	Softmax	1*1*1000	0
25	output	Classification Output	-	0

3.7 Matching and Decision

3.7.1 Softmax Layer

The input values that entered may be negative, positive, zero, or greater than one. This function converts the entered values between one and zero so that they can be interpreted as probabilities. If the input is small or negative, it turns it into a small probability, and if the input is large or positive, it turns it into a high probability, but it will always remain between zero and one.

3.7.2 Loss function

The loss function is used to determine loss (error) in each trading period or epoch, which is also an important factor on which to update weight during backpropagation. It explains the difference between expected outputs and real labeling.

Chapter 4 – Experimental result and discussion of the proposed system

Chapter Four

Experimental result and discussion of the proposed system

4.1 Introduction

The proposed system is designed to identify people who use the most important biometric characteristics, which is a palm print, by identifying people from the pattern of the veins in the palm by using the CASIA database. The identification of people through veins is one of the most important vital measures because of the different patterns of each person. Even identical twins have a different pattern, and this pattern is constant even with advanced age. After processing, the hand image in feature extraction and extracting the pattern. The pattern moves across the convolution neural network to ensure that the best feature, matching, and decision are extracted.

In this chapter, the experimental results of preprocessing, extraction of patterns, and CNN for the proposed system will be clarified.

4.2 System Requirements

Any system needs some specific requirements to get the best result. The requirements of the Hardware and Software are necessary for this system to facilitate and make it work fast.

4.2.1 Hardware Requirements

Laptop computer with following specifications:-

1. Intel(R) Core(TM) i7-8565U
2. RAM 16 Gigabyte
3. Hard 1 Terabyte with Hard 500-Gigabyte m.2

4. VGA 4 Gigabyte

4.2.2 Software Requirements

This system has been implemented on the 10 windows. Matlab 2020a. The proposed system was implemented using Matlab for the preprocessing of images, the extraction of patterns, and the construction of CNN designed for the proposed work.

4.3 Test and Implementation

The system provided was a test using the CASIA Multi-Spectral Palm-print Image Dataset with 7200 images of 100 different people. This will be explained in detail in appendix A.

4.4 Dataset

The data that used in our thesis contains 7,200 images taken of 100 different people with both hands using the multispectral camera. As shown in Figure (4.1) the images are an 8-bit gray-level jpeg. For each hand, images were taken in two different sessions, the interval between them was more than a month. Each session contains three samples. Each sample contains six images of palms that took at the same time and in six different wavelengths, which are 940nm, 850nm, 700nm, 630nm, 460nm in addition to the white color.

The device provides equally distributed lighting and pictures taken using a CCD camera in the lower part of the device. design a circle to control the spectrum automatically. Figure (4.2) shows six typical handprint images in the database and the figure (4.1) shows the multispectral imaging device[62].

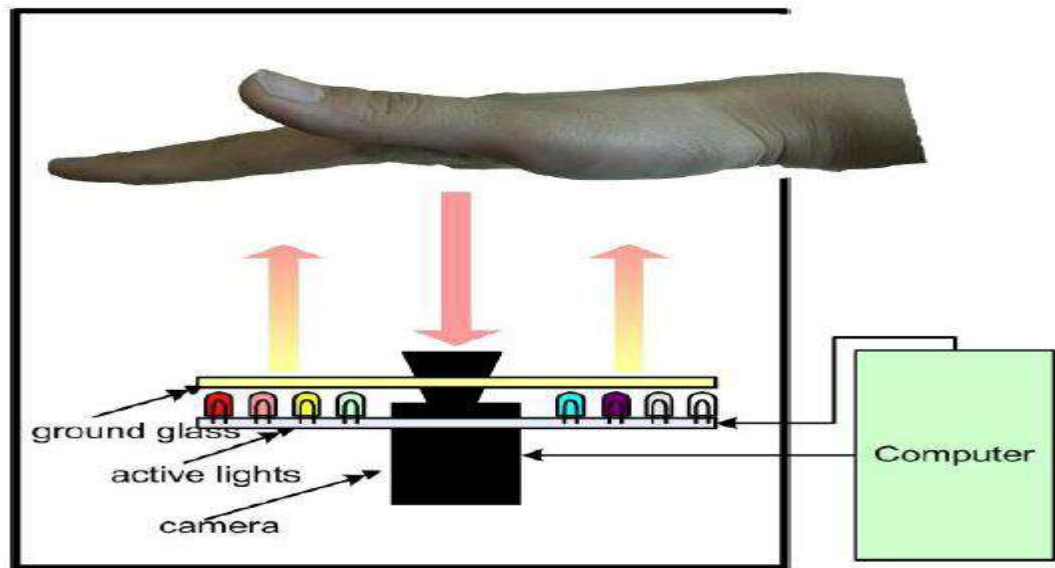


Figure (4.1): Multispectral imaging device

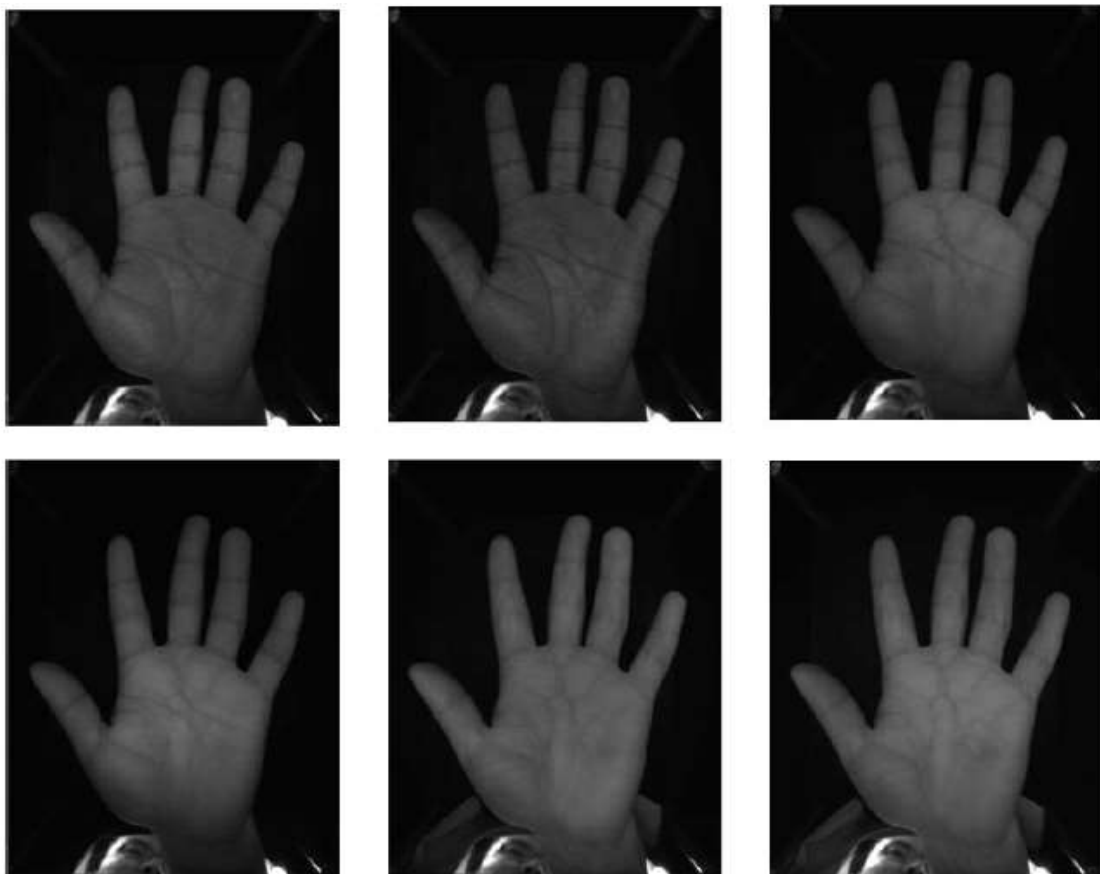


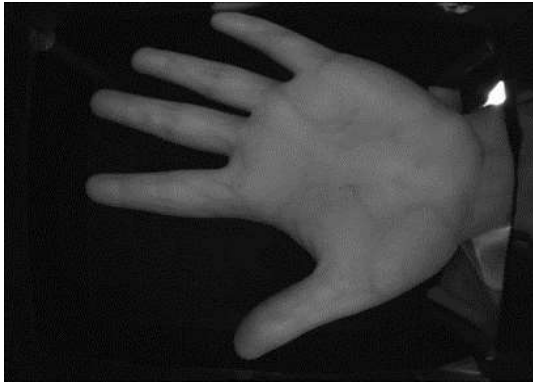
Figure (4.2): six images of Palmprint from the dataset

4.5 Experimental Result of the Proposed System

Considering that the proposed system exists by identifying people through the vein in the palm, and by creating a fast and strong system, the choice of this biometric was important. The remainder of this chapter will illustrate the outputs of each step in the proposed system.

4.5.1 Preprocessing Stage

To extract the features of good performance for each person, it must be discovery and the return on the region of interest in which the veins are concentrated in this region. Apply a set of processes to achieve this result as shown in figure (4.3). In the first process, rotate the images in the database CASIA. Most of the images were taken in different directions, so rotated them until they were all equal, and then carried out the process of converting the image into a binary image by the binarization process and then removed the noise around the palm. Therefore, cropping the palm from the background because there were some unimportant things in the image, then extracted the important boundaries that need in the image and then identified the important points to draw the important area that contains veins. After extracting the ROI, showed an image that contains noise, so applied some filters to improve the image. Initially, implemented the median filter. Then applied the anisotropic diffusion filter, then the closing operation filter, and then extracted the pattern to insert it into the CNN.



a



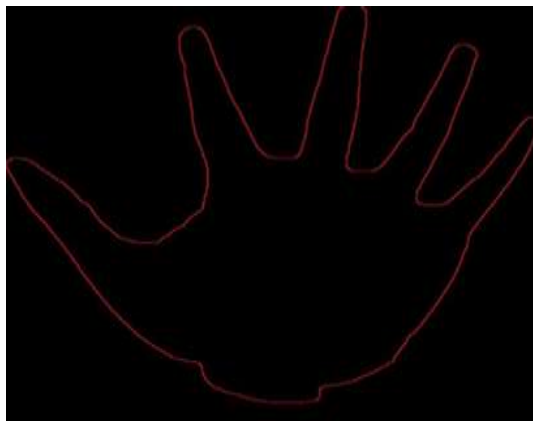
b



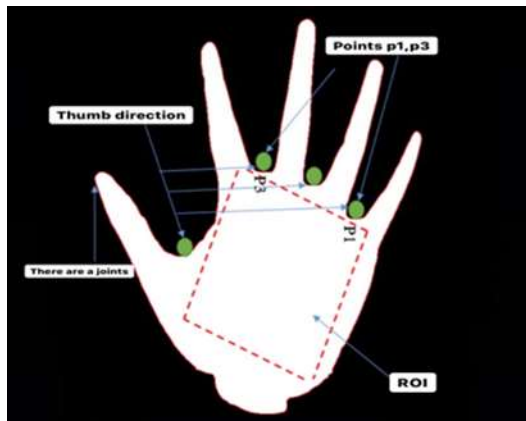
c



d



e



f

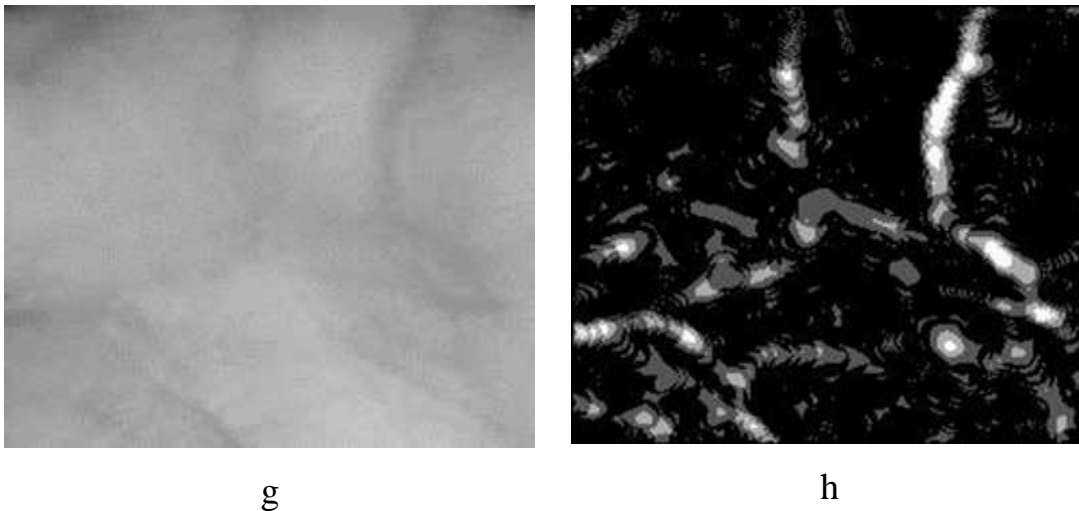


Figure (4.3): steps of preprocessing stage (a) The original image (b) Rotation image (c) Binary image (d) Noise removal (e) Boundary extraction (f) Determine ROI (g) ROI extraction (h) pattern extraction

4.5.2 Convolutional Neural Network (CNN)

CNN is a subset (category) of an artificial neural network (ANN), which is usually used to compile, classify, identify, and analyses visual images. CNN offers a more robust extraction, matching, and decision-making advantage than traditional algorithms. It is therefore widely used in the pattern, the identification of faces, and the identification of biometrics in general. CNN consists of one input layer, one output layer, and many hidden layers. The input image goes between layers to extract the features, then match and make a decision.

4.5.2.1 Feature Extraction

Feature extraction is the core of the identification system. The convolutional layer (conv_1) in CNN is the feature extraction layer, and it works by moving the weight mask over the input image and doing multiplication of the raster product. The result is called a feature map, and a feature map from the first convolutional layer (conv_1) acts as an input to

the batch normalization layer (normal batch_1) that reduces the numbers of the features map (the numbers that represent the input image after the convolutional layer 1) to speed up the training process. The next layer is RleU, which ignores the negative number to ensure only the vital features remain, so the features map is minimized.

4.5.2.2 Matching and Decision

After the completion of the training process, it must be the test process. Application for identification performance. Because the result of the feature extraction layer pass to a fully connected layer (FC). Which links each nerve cell in one layer to all neuro cells in the other layer, this layer takes the feature of making an initial classification by increasing and reducing the figure corresponding to the candidate category, FC moves to the Softmax layer, which gives the result.

4.6 Training and Test Validation

As mentioned above, the database that used in our work consists of 7200 images and contains six wavelengths, each wave spectrum contains 600 images for the left and right hand. In our work, working on the entire database in addition to working on each band separately. Divided the data into three cases. The first case is when the test and verification ratio is 50/50, the second case is when the ratio is 70/30, and the third case is when it is 90/10.

Table 4-1 Split of the database image

Number of images	Training	Test and validation	percentage
600	300	300	50/50
600	400	200	70/30
600	500	100	90/10
7200	3600	3600	50/50
7200	5040	2160	70/30
7200	6480	720	90/10

4.7 Result and Discussion of Palm Vein Identification Based on proposed CNN

The dataset CASIA palm image was implemented. It contains 100 people with six samples of each palm (left and right hand). In addition, divided the data into 100 classes, and each class contains six images for each band, where the number of images for each band was 600 from the six bands and for both hands. However, when used the entire database was used all 7200 images, each class contained 72 images. The training was conducted with 20 epoch, and a learning rate of 0.01 for each band. In addition, when used all the images in the database, the number of iteration was 560 for case 50/50, 780 iterations for case 70/30, and 1000 iteration for case 90/10.

Table (4.2) provides detailed information about training data for the band 850L. Where the percentage training is 90 and percentage testing 10 based on proposed CNN. Epoch = number of periods for all samples in the dataset, where iteration = number of periods per sample training, time elapse

= time spent for sample training, mini-batch accuracy = accuracy training for each sample, and the learning rate is training rate

Table 4-2 the details of layer for our proposed CNN

Layer	Name	Type	Activation	Learnable
1	Input	Image input	32*32*1	-
2	Conv_1	Convolution	32*32*16	Weight 23*23*1*16 Bias 1*1*16
3	BN_1	Batch normalization	32*32*16	Offset 1*1*16 Scale 1*1*16
4	Relu_1	ReLU	32*32*16	
5	Conv_2	Convolution	16*16*64	Weight 23*23*16*64 Bias 1*1*64
6	BN_2	Batch normalization	16*16*64	Offset 1*1*64 Scale 1*1*64
7	Relu_2	ReLU	16*16*64	
8	Conv_3	Convolution	16*16*32	Weight 23*23*64*32 Bias 1*1*32
9	BN_3	Batch normalization	16*16*32	Offset 1*1*32 Scale 1*1*32
10	Relu_3	ReLU	16*16*32	
11	Avpool	Average pooling	8*8*32	
12	Fc	Fully connected	1*1*100	Weight 100*2048 Bias 1*100
13	Softmax2	Softmax	1*1*100	-
14	Class output	Classification output	-	-

Table 4-3 Details information of data training about 850L using proposed CNN

Epoch	Iteration	Time elapse	accuracy validation	Learning rate
1	7	00:00:08	54	0.01
3	21	00:00:20	91	0.01
5	35	00:00:37	96	0.01
7	49	00:00:53	97	0.01
9	63	00:01:06	98	0.01
11	77	00:01:22	98	0.01
13	91	00:01:34	98	0.01
15	105	00:01:52	98	0.01
17	119	00:01:58	98	0.01
20	120	00:02:16	98	0.01

Table 4-4 Accuracy of the band 460 nm

Name Of band	Number of Palms	Number of person	Number Of sample	Training percentage	Testing percentage	Performance of proposed CNN				
						AV	F-S	Pr	Se	Sp
460L	600	100	6	50%	50%	61%	58.86%	66.49%	61%	99.61%
460L	600	100	6	70%	30%	62.50%	59.81%	66%	62.50%	99.62%
460L	600	100	6	90%	10%	69%	63.33%	70.17%	69%	99.69%
460R	600	100	6	50%	50%	62.88%	58.70%	65.25%	61.44%	99.62%
460R	600	100	6	70%	30%	72.09	67.80%	73.43%	71.34%	99.72%
460R	600	100	6	90%	10%	83.65	78.33%	83%	83%	99.83%

Table 4-5 Accuracy of the band 630 nm

Name Of band	Number of Palms	Number of person	Number Of sample	Training percentage	Testing percentage	Performance of proposed CNN				
						AV	F-S	Pr	Se	Sp
630L	600	100	6	50%	50%	92.13%	90.90%	92.73%	92.21%	99.92%
630L	600	100	6	70%	30%	92.12%	90.94%	93%	92%	99.92%
630L	600	100	6	90%	10%	97.03%	96.13%	97.17%	97%	99.97%
630R	600	100	6	50%	50%	90.99%	89.43%	93.13%	90%	99.91%
630R	600	100	6	70%	30%	93.64%	92.43%	94.17%	93%	99.94%
630R	600	100	6	90%	10%	91.51%	88.60%	91.38%	91%	99.91%

Table 4-6 Accuracy of the band 700 nm

Name Of band	Number of Palms	Number of person	Number Of sample	Training percentage	Testing percentage	Performance of proposed CNN				
						AV	F-S	Pr	Se	Sp
700L	600	100	6	50%	50%	90%	89.53%	92.30%	90%	99.90%
700L	600	100	6	70%	30%	94%	93.47%	96%	94%	99.94%
700L	600	100	6	90%	10%	97%	96%	97%	97%	99.97%
700R	600	100	6	50%	50%	88.33%	87.01%	89.88%	88.33%	99.88%
700R	600	100	6	70%	30%	93%	92.30%	94.83%	93%	99.93%
700R	600	100	6	90%	10%	94%	92%	94%	94%	99.94%

Table 4-7 Accuracy of the band 850 nm

Name Of band	Number of Palms	Number of person	Number Of sample	Training percentage	Testing percentage	Performance of proposed CNN				
						AV	F-S	Pr	Se	Sp
850L	600	100	6	50%	50%	97%	96.83%	97.58%	97%	99.97%
850L	600	100	6	70%	30%	97.50%	97.33%	98.50%	97.50%	99.97%
850L	600	100	6	90%	10%	98%	97.33%	98%	98%	99.98%
850R	600	100	6	50%	50%	96%	95.85%	96.92%	96%	99.96%
850R	600	100	6	70%	30%	97%	96.50%	97.33%	97%	99.97%
850R	600	100	6	90%	10%	99%	98.67%	99%	99%	99.99%

Table 4-8 Accuracy of the band 940 nm

Name Of band	Number of Palms	Number of person	Number Of sample	Training percentage	Testing percentage	Performance of proposed CNN				
						AV	F-S	Pr	Se	Sp
940L	600	100	6	50%	50%	95.33%	94.86%	95.85%	95.33%	99.95%
940L	600	100	6	70%	30%	96.50%	96.30%	97.50%	96.50%	99.96%
940L	600	100	6	90%	10%	97%	96%	97%	97%	99.97%
940R	600	100	6	50%	50%	92%	91.57%	92.82%	92%	99.92%
940R	600	100	6	70%	30%	93.50%	92.83%	93.83%	93.50%	99.93%
940R	600	100	6	90%	10%	94%	93%	94%	94%	99.94%

Table 4-9 Accuracy of the band WHT nm

Name Of band	Number of Palms	Number of person	Number Of sample	Training percentage	Testing percentage	Performance of proposed CNN				
						AV	F-S	Pr	Se	Sp
WHTL	600	100	6	50%	50%	89%	87.80%	90.66%	89%	99.89%
WHTL	600	100	6	70%	30%	93%	92.17%	95.07%	93%	99.93%
WHTL	600	100	6	90%	10%	84.85%	80%	84.50%	84.85%	99.85%
WHTR	600	100	6	50%	50%	81.61%	79.85%	83.84%	81.33%	99.81%
WHTR	600	100	6	70%	30%	83.92%	82.18%	85.80%	83.50%	99.84%
WHTR	600	100	6	90%	10%	84.85%	80%	84.50%	84.85%	99.85%

Table 4-10 Accuracy of all data

Name Of band	Number of Palms	Number of person	Number Of sample	Training percentage	Testing percentage	Performance of proposed CNN				
						AV	F-S	Pr	Se	Sp
All data	600	100	6	50%	50%	92.53%	92.54%	92.80%	92.52%	99.92%
All data	600	100	6	70%	30%	93.59%	93.62%	93.99%	93.59%	99.94%
All data	600	100	6	90%	10%	94.43%	94.42%	94.43%	94.43%	99.94%

4.8 Result and Discussion of Palm Vein Identification Based on AlexNet

Table (4.9) provides detailed information about training data for the band 850L. Where the percentage training is 90 and percentage testing 10 based on the proposed AlexNet. Epoch = number of periods for all samples in the dataset, where iteration = number of periods per sample training, time elapse = time spent for sample training, mini-batch accuracy = accuracy training for each sample, and the learning rate is training rate.

Table 4-11 Details information of data training about 850L using AlexNet

Epoch	Iteration	Time elapse	accuracy validation	Learning rate
1	50	00:00:43	3	0.0001
10	500	00:06:08	78	0.0001
20	1000	00:12:44	90	0.0001
30	1500	00:18:32	90	0.0001
40	2000	00:24:48	91	0.0001
50	2500	00:30:29	91	0.0001
60	3000	00:37:10	91	0.0001
70	3500	00:43:32	94	0.0001
90	4500	01:04:14	94	0.0001
100	5000	01:11:03	96	0.0001

Table 4-12 Accuracy of the band 460 nm

Name Of band	Number of Palms	Number of person	Number Of sample	Training percentage	Testing percentage	Performance of AlexNet				
						AV	F-S	Pr	Se	Sp
460L	600	100	6	50%	50%	62.67%	59.32%	64.58%	64.67%	99.62%
460L	600	100	6	70%	30%	74.50%	74.94%	83.32%	74.50%	99.74%
460L	600	100	6	90%	10%	78%	72.07%	79.42%	78%	99.78%
460R	600	100	6	50%	50%	66.87%	62.44%	71.09%	64.66%	99.66%
460R	600	100	6	70%	30%	76.28%	73.42%	81.39%	75.61%	99.76%
460R	600	100	6	90%	10%	79.81%	73.50%	80%	79%	99.80%

Table 4-13 Accuracy of the band 630 nm

Name Of band	Number of Palms	Number of person	Number Of sample	Training percentage	Testing percentage	Performance of AlexNet				
						AV	F-S	Pr	Se	Sp
630L	600	100	6	50%	50%	84.59%	82.84%	87.45%	84.45%	99.84%
630L	600	100	6	70%	30%	97.04%	96.47%	97.50%	97%	99.97%
630L	600	100	6	90%	10%	92.08%	89.50%	92.33%	92%	99.92%
630R	600	100	6	50%	50%	88.89%	86.77%	90.28%	87.97%	99.89%
630R	600	100	6	70%	30%	94.09%	93.09%	95.75%	93.50%	99.94%
630R	600	100	6	90%	10%	92.45%	89.33%	92%	92%	99.92%

Table 4-14 Accuracy of the band 700 nm

Name Of band	Number of Palms	Number of person	Number Of sample	Training percentage	Testing percentage	Performance of AlexNet				
						AV	F-S	Pr	Se	Sp
700L	600	100	6	50%	50%	77.67%	76.34%	82.52%	77.67%	99.77%
700L	600	100	6	70%	30%	91%	90.67%	93%	91%	99.91%
700L	600	100	6	90%	10%	88%	84.33%	88%	88%	99.88%
700R	600	100	6	50%	50%	81%	79.35%	83.22%	81%	99.81%
700R	600	100	6	70%	30%	90.50%	89%	92%	90.50%	99.90%
700R	600	100	6	90%	10%	88%	84%	88%	88%	99.88%

Table 4-15 Accuracy of the band 850 nm

Name Of band	Number of Palms	Number of person	Number Of sample	Training percentage	Testing percentage	Performance of AlexNet				
						AV	F-S	Pr	Se	Sp
850L	600	100	6	50%	50%	87.33%	86.14%	88.67%	87.33%	99.87%
850L	600	100	6	70%	30%	91%	89.90%	91.83%	91%	99.91%
850L	600	100	6	90%	10%	96%	94.67%	96%	96%	99.96%
850R	600	100	6	50%	50%	90.33%	89.62%	91.87%	90.33%	99.90%
850R	600	100	6	70%	30%	94%	93.43%	95.67%	94%	99.94%
850R	600	100	6	90%	10%	96%	94.67%	96%	96%	99.96%

Table 4-16 Accuracy of the band 940 nm

Name Of band	Number of Palms	Number of person	Number Of sample	Training percentage	Testing percentage	Performa Performance of AlexNet				
						AV	F-S	Pr	Se	Sp
940L	600	100	6	50%	50%	89.67%	88.93%	92.40%	89.67%	99.90%
940L	600	100	6	70%	30%	95%	94.80%	96.50%	95%	99.95%
940L	600	100	6	90%	10%	96%	94.67%	96%	96%	99.96%
940R	600	100	6	50%	50%	88.33%	87.98%	90.62%	88.33%	99.88%
940R	600	100	6	70%	30%	91.50	90.75%	93.33%	91.50	99.91%
940R	600	100	6	90%	10%	91%	89.50%	91.83%	91%	99.91%

Table 4-17 Accuracy of the band WHT nm

Name Of band	Number of Palms	Number of person	Number Of sample	Training percentage	Testing percentage	Performance of AlexNet				
						AV	F-S	Pr	Se	Sp
WHTL	600	100	6	50%	50%	83.67%	82.31%	86.02%	83.67%	99.84%
WHTL	600	100	6	70%	30%	91%	90.10%	93.83%	91%	99.91%
WHTL	600	100	6	90%	10%	97%	96%	97%	97%	99.97%
WHTR	600	100	6	50%	50%	78.60%	77.04%	82.03%	78.33%	99.78%
WHTR	600	100	6	70%	30%	81.91%	79.77%	83.92%	81.91%	99.82%
WHTR	600	100	6	90%	10%	81.82%	77.67%	82.67%	81.82%	99.82%

Table 4-18 Accuracy of all data

Name Of band	Number of Palms	Number of person	Number Of sample	Training percentage	Testing percentage	Performance of AlexNet				
						AV	F-S	Pr	Se	Sp
All data	7200	100	6	50%	50%	83.77%	83.94%	86.15%	83.77%	99.84%
All data	7200	100	6	70%	30%	92.45%	92.41%	93.06%	92.45%	99.92%
All data	7200	100	6	90%	10%	93%	92.93%	93.90%	93%	99.93%

Work was done on all the waveforms in the database, where the data was divided in the training phase after extracting the pattern, as it was entered into the proposed CNN and the AlexNet.

The data was divided into three cases: 50/50, 70/30, and 90/10. Our proposed network was superior to AlexNet in terms of accuracy and training time 99% is obtained at the 850nm band when the training ratio is 90/10, which corresponds to 96% in the Alexnet network.

Chapter 5 – Conclusion and future direction

Chapter 5

Conclusion and Future Directions

5.1 Conclusion

Many of the conclusions can be drawn from and discussed, summarized as follows.

The method of border removal, which is a method of disposing of hand limits, is that the system does not even think about borders as part of the vein, so it gives a clear and the mode of the vein understandable.

The approach to the extraction of the region of interest in the palm print has been introduced, to obtain an important part of the palm print (which contains baselines and permanent) and to liberate the other part, and conclude less time and less mathematical account for the next process.

CNN is one of the techniques used for classification and consists of several layers, usually (convolution layer, batch normalization layer, ReLU activation layer). A fully connected layer and a softmax layer, but in this system the Batch Normalization layer is used to accelerate the training process. Conclude that the system takes less time and this is a very important feature.

Our work has also been tested on the global AlexNet network, which is trained on more than a million images from ImageNet. Therefore,

Compare the results with our proposed network in terms of accuracy and time.

The database that we worked on contains six wave spectra. Work has been done on each wave spectrum separately. In addition, they all worked together. Each wave spectrum contains 600 images for the right hand and 600 images for the left hand. 7200 images for all data. The images were divided into 100 rows according to the number of people. Each wave spectrum was segmented and its resolution extracted by three cases. The first case is when the training and testing ratio is 50/50, the second case when the training and testing ratio is 70/30, and the last case when it is 90/10.

5.2 Future Directions

1. Built a multimodal system based on palm vein and palm print or any two biometric models.
2. Implementation of an Application of a unimodal system based on CNN in real-time such as the bank and/or Master Card, etc.
3. Proposed a new neural convolution network.
4. Construction database of palm prints containing millions of images.

References

References

- [1] P. Sareen, "Biometrics—introduction, characteristics, basic technique, its types and various performance measures," *Int J Emerg Res Manag Technol*, vol. 3, pp. 109–119, 2014.
- [2] A. K. Jain, A. Ross, and S. Prabhakar, "An Introduction to Biometric Recognition," *IEEE Trans. Circuits Syst. Video Technol.*, vol. 14, no. 1, pp. 4–20, 2004, doi: 10.1109/TCSVT.2003.818349.
- [3] N. K. Ratha, J. H. Connell, and R. M. Bolle, "Enhancing security and privacy in biometrics-based authentication systems," *IBM Syst. J.*, vol. 40, no. 3, pp. 614–634, 2001.
- [4] P. D. Deshpande, A. S. Tavildar, Y. H. Dandwate, and E. Shah, "Fusion of dorsal palm vein and palm print modalities for higher security applications," in *2016 Conference on Advances in Signal Processing (CASP)*, 2016, pp. 201–206.
- [5] Y. H. Dandawate and S. R. Inamdar, "Fusion based multimodal biometric cryptosystem," in *2015 International Conference on Industrial Instrumentation and Control (ICIC)*, 2015, pp. 1484–1489.
- [6] M. A. Ahmed, H. M. Ebied, E.- Sayed, M. El-Horbaty, and A.-B. M. Salem, "Analysis of Palm Vein Pattern Recognition Algorithms and Systems," *2013*, Accessed: Nov. 19, 2021. [Online]. Available: <http://citeseerx.ist.psu.edu/viewdoc/summary?doi=10.1.1.380.388>.
- [7] K. Deepti and R. Krishnaiah, "Palm Vein Technology," *Int. J. Comput. Eng. & Appl.*, vol. 11, no. 1, 2013.
- [8] M. G.- IJCST and undefined 2011, "Morphological image processing," *Citeseer*, Accessed: Nov. 19, 2021. [Online]. Available: <http://citeseerx.ist.psu.edu/viewdoc/download?doi=10.1.1.219.4602&rep=rep1&type=pdf>.
- [9] K. R. preprint arXiv:1312.6219 and undefined 2013, "Extracting region of interest

for palm print authentication,” *arxiv.org*, Accessed: Nov. 19, 2021. [Online]. Available: <https://arxiv.org/abs/1312.6219>.

- [10] R. Yogamangalam, B. K.-I. J. of, and undefined 2013, “Segmentation techniques comparison in image processing,” *faratarjome.ir*, Accessed: Nov. 19, 2021. [Online]. Available: http://faratarjome.ir/u/media/shopping_files/store-EN-1485851260-5979.pdf.
- [11] S. Matta, “Various image segmentation techniques,” *Int. J. Comput. Sci. Inf. Technol.*, vol. 5, no. 6, pp. 7536–7539, 2014.
- [12] V. Bhosale, S. Kale, M. Pawar, ... R. P.-I. J. of, and undefined 2014, “Palm. Vein Extraction and Matching For Personal Identification,” *academia.edu*, Accessed: Nov. 19, 2021. [Online]. Available: https://www.academia.edu/download/36671015/publish_paper.pdf.
- [13] M. Rajalakshmi, V. Ganapathy, and R. Rengaraj, “Palm-dorsal vein pattern authentication using convoluted neural network (CNN),” *Int. J. Pure Appl. Math.*, vol. 116, no. 23, pp. 525–532, 2017.
- [14] D. Thapar, G. Jaswal, A. Nigam, and V. Kanhangad, “PVSNet: Palm Vein Authentication Siamese Network Trained using Triplet Loss and Adaptive Hard Mining by Learning Enforced Domain Specific Features,” *ISBA 2019 - 5th IEEE Int. Conf. Identity, Secur. Behav. Anal.*, pp. 1–8, 2019, doi: 10.1109/ISBA.2019.8778623.
- [15] S. Chantaf, A. Hilal, and R. Elsaleh, “Palm Vein Biometric Authentication Using Convolutional Neural Networks,” *Smart Innov. Syst. Technol.*, vol. 146, pp. 352–363, 2020, doi: 10.1007/978-3-030-21005-2_34.
- [16] S. Y. Jhong *et al.*, “An automated biometric identification system using CNN-based palm vein recognition,” *Int. Conf. Adv. Robot. Intell. Syst. ARIS*, vol. 2020-Augus, 2020, doi: 10.1109/ARIS50834.2020.9205778.
- [17] M. ELRASHEED, “DESIGN AND IMPLEMENTATION OF CLAIM BASED BIOMETRIC AUTHENTICATION SYSTEM OVER THE CLOUD.”

- [18] E. Q. Naamha, "Fingerprint Identification and Verification System Based on Extraction of Unique ID," *PhD diss., Univ. Technol.*, 2017.
- [19] J. R. Vacca, *Biometric technologies and verification systems*. Elsevier, 2007.
- [20] L. Dian and S. Dongmei, "Contactless palmprint recognition based on convolutional neural network," in *2016 IEEE 13th International Conference on Signal Processing (ICSP)*, 2016, pp. 1363–1367.
- [21] Z. M. Noh, A. R. Ramli, M. Iqbal Saripan, and M. Hanafi, "Overview and challenges of palm vein biometric system," *Int. J. Biom.*, vol. 8, no. 1, pp. 2–18, 2016, doi: 10.1504/IJBM.2016.077102.
- [22] A. W. K. Kong and D. Zhang, "Feature-level fusion for effective palmprint authentication," *Lect. Notes Comput. Sci. (including Subser. Lect. Notes Artif. Intell. Lect. Notes Bioinformatics)*, vol. 3072, pp. 761–767, 2004, doi: 10.1007/978-3-540-25948-0_103.
- [23] Y.-P. Lee, "Palm vein recognition based on a modified [formula]," *Signal, image video Process.*, vol. 9, no. 1, pp. 229–242, 2015.
- [24] R. Anderson, J. P.-J. of investigative dermatology, and undefined 1981, "The optics of human skin," *Elsevier*, Accessed: Nov. 19, 2021. [Online]. Available: <https://www.sciencedirect.com/science/article/pii/S0022202X15461251>.
- [25] Y. B. Zhang, Q. Li, J. You, and P. Bhattacharya, "Palm vein extraction and matching for personal authentication," *Lect. Notes Comput. Sci. (including Subser. Lect. Notes Artif. Intell. Lect. Notes Bioinformatics)*, vol. 4781 LNCS, pp. 154–164, 2007, doi: 10.1007/978-3-540-76414-4_16.
- [26] H. Zhang and D. Hu, "A palm vein recognition system," in *2010 International Conference on Intelligent Computation Technology and Automation*, 2010, vol. 1, pp. 285–288.
- [27] G. K. O. Michael, T. Connie, L. S. Hoe, and A. T. B. Jin, "Design and implementation of a contactless palm vein recognition system," in *Proceedings of the 2010 Symposium on Information and Communication Technology*, 2010, pp.

92–99.

- [28] M. Greitans, M. Pudzs, and R. Fuksis, “Palm vein biometrics based on infrared imaging and complex matched filtering,” in *Proceedings of the 12th ACM Workshop on Multimedia and Security*, 2010, pp. 101–106.
- [29] M. Kowalski and others, “Vein pattern database and benchmark results (Image and vision processing and display technology),” *Electron. Lett.*, vol. 47, no. 20, pp. 1127–1128, 2011.
- [30] W.-Y. Han and J.-C. Lee, “Palm vein recognition using adaptive Gabor filter,” *Expert Syst. Appl.*, vol. 39, no. 18, pp. 13225–13234, 2012.
- [31] P. Tome and S. Marcel, “On the vulnerability of palm vein recognition to spoofing attacks,” in *2015 International Conference on Biometrics (ICB)*, 2015, pp. 319–325.
- [32] P.-O. Ladoux, C. Rosenberger, and B. Dorizzi, “Palm vein verification system based on SIFT matching,” in *International Conference on Biometrics*, 2009, pp. 1290–1298.
- [33] P. Cancian, G. W. Di Donato, V. Rana, and M. D. Santambrogio, “An embedded Gabor-based palm vein recognition system,” in *2017 IEEE EMBS International Conference on Biomedical & Health Informatics (BHI)*, 2017, pp. 405–408.
- [34] A. Sierro, P. Ferrez, and P. Roudit, “Contact-less palm/finger vein biometrics,” in *2015 International Conference of the Biometrics Special Interest Group (BIOSIG)*, 2015, pp. 1–12.
- [35] J. Cao, M. Xu, W. Shi, Z. Yu, A. Salim, and P. Kilgore, “MyPalmVein: a palm vein-based low-cost mobile identification system for wide age range,” in *2015 17th International Conference on E-health Networking, Application & Services (HealthCom)*, 2015, pp. 292–297.
- [36] A. F. Akbar, T. A. B. Wirayudha, and M. D. Sulistiyo, “Palm vein biometric identification system using local derivative pattern,” *2016 4th Int. Conf. Inf. Commun. Technol. ICoICT 2016*, vol. 4, no. c, 2016, doi:

10.1109/ICoICT.2016.7571956.

- [37] Y. H. Ali and Z. N. Razuqi, "Palm vein recognition based on centerline," *Iraqi J Sci*, vol. 58, no. 2A, pp. 726–734, 2017.
- [38] P. Tome and S. Marcel, "Palm vein database and experimental framework for reproducible research," in *2015 International Conference of the Biometrics Special Interest Group (BIOSIG)*, 2015, pp. 1–7.
- [39] W. Kang and Q. Wu, "Contactless palm vein recognition using a mutual foreground-based local binary pattern," *IEEE Trans. Inf. Forensics Secur.*, vol. 9, no. 11, pp. 1974–1985, 2014.
- [40] J.-C. Lee, "A novel biometric system based on palm vein image," *Pattern Recognit. Lett.*, vol. 33, no. 12, pp. 1520–1528, 2012.
- [41] Y.-B. Zhang, Q. Li, J. You, and P. Bhattacharya, "Palm vein extraction and matching for personal authentication," in *International Conference on Advances in Visual Information Systems*, 2007, pp. 154–164.
- [42] S. Lin, "Low-cost biometric recognition system based on NIR palm vein image," no. November 2018, 2020, doi: 10.1049/iet-bmt.2018.5027.
- [43] H.D., B.S., E. J.-M. NS. NS. 2008 - spiedigitallibrary.org, "A comparative analysis of the body based on a person's appearance to confess," Accessed: Nov. 19, 2021. [Online]. Available: <https://www.spiedigitallibrary.org/journals/journal-of-electronic-imaging/volume-17/issue-1/011018/Comparative-analysis-of-global-hand-appearance-based-person-recognition/10.1117/1.2890986.short>.
- [44] "Robust Classification With Convolutional," no. May, 2015.
- [45] B. O. Zapletal, *Image recognition by convolutional neural networks - basic concepts*. 2017.
- [46] S. Chantaf, A. Hilal, and R. Elsaleh, *Palm Vein Biometric Authentication Using Convolutional Neural Networks*, vol. 146. Springer International Publishing, 2020.
- [47] J. Vojt, "Deep neural networks and their implementation," 2016.

- [48] H. I. Abdulrazzaq, "Robust Authorization Based on Multi Biometric Techniques," 2018.
- [49] N. Mattsson, "Classification Performance of Convolutional Neural Networks," no. 16060, p. 46, 2016.
- [50] E. Calli, "Faster Convolutional Neural Networks," p. 11, 2017, [Online]. Available:
https://theses.uhn.nl/bitstream/handle/123456789/5233/Calli%2C_E._1.pdf?sequence=1.
- [51] Z. Z.-U. of Tennessee, undefined Knoxville, undefined TN, and undefined 2016, "Derivation of backpropagation in convolutional neural network (cnn)," *zzutk.github.io*, doi: 10.1109/MSP.2012.2205597.
- [52] M. Dixit, R. Jayaswal, and M. Dixit, "A Comparative Analysis of Human Facial Recognition by Conventional Methods and Deep Learning in Real Time Environment," 2020 IEEE 9 International Conference..., 2020 - ieeexplore.ieee.org, 2020, doi : 10.1109/CSNT.2020.13.
- [53] G. Hinton *et al.*, "Deep neural networks for acoustic modeling in speech recognition: The shared views of four research groups," *IEEE Signal Process. Mag.*, vol. 29, no. 6, pp. 82–97, 2012.
- [54] A. S. Al-Waisy, R. Qahwaji, S. Ipson, S. Al-Fahdawi, and T. A. M. Nagem, "A multi-biometric iris recognition system based on a deep learning approach," *Pattern Anal. Appl.*, vol. 21, no. 3, pp. 783–802, 2018, doi: 10.1007/s10044-017-0656-1.
- [55] A. S. Al-Waisy, R. Qahwaji, S. Ipson, S. Al-Fahdawi, and T. A. M. Nagem, "A multi-biometric iris recognition system based on a deep learning approach," *Pattern Anal. Appl.*, vol. 21, no. 3, pp. 783–802, 2018.
- [56] M. Thoma, "Analysis and Optimization of Convolutional Neural Network Architectures," Jul. 2017, Accessed: Nov. 19, 2021. [Online]. Available: <http://arxiv.org/abs/1707.09725>.

- [57] C. Laurent, G. Pereyra, P. Brakel, Y. Zhang, and Y. Bengio, "Batch normalized recurrent neural networks," in *2016 IEEE International Conference on Acoustics, Speech and Signal Processing (ICASSP)*, 2016, pp. 2657–2661.
- [58] J.-C. Chen, V. M. Patel, and R. Chellappa, "Unconstrained face verification using deep cnn features," in *2016 IEEE winter conference on applications of computer vision (WACV)*, 2016, pp. 1–9.
- [59] Y. Yu and S. T. Acton, "Speckle reducing anisotropic diffusion," *IEEE Trans. image Process.*, vol. 11, no. 11, pp. 1260–1270, 2002.
- [60] A. McAndrew, "An introduction to digital image processing with matlab notes for scm2511 image processing," *Sch. Comput. Sci. Math. Victoria Univ. Technol.*, vol. 264, no. 1, pp. 1–264, 2004.
- [61] V. B. Langote and D. S. Chaudhari, "Segmentation techniques for image analysis," *Int. J. Adv. Eng. Res. Stud.*, vol. 1, no. 2, pp. 252–255, 2012.
- [62] C. M. Palmprint and I. Database, "Note on CASIA Multi-Spectral Palmprint Database," pp. 1–4.

Appendices

Appendix A

Multiple Spectral Image Details

The data set is using self-designed multiple spectral imaging devices, as shown in Figure (4.1). All palm images are 8-bit gray-level JPEG files. For each hand, capture two sessions of palm images. The time interval between the two sessions is more than one month. In each session, there are three samples. Each sample contains six palm images, which are captured at the same time with six different electromagnetic spectrums. Wavelengths of the illuminator corresponding to the six spectra are 460nm, 630nm, 700nm, 850nm, 940nm, and white light respectively. Between two samples, allow a certain degree of variations of hand postures. Through that, aim to increase the diversity of intra-class samples and simulate practical use. In this device, there are no pegs to restrict postures and positions of palms. Subjects are required to put their palm into the device and lay it before a uniform-colored background. The device supplies an evenly distributed illumination and captures palm images using a CCD camera fixed on the bottom of the device and design a control circuit to adjust spectrums automatically.

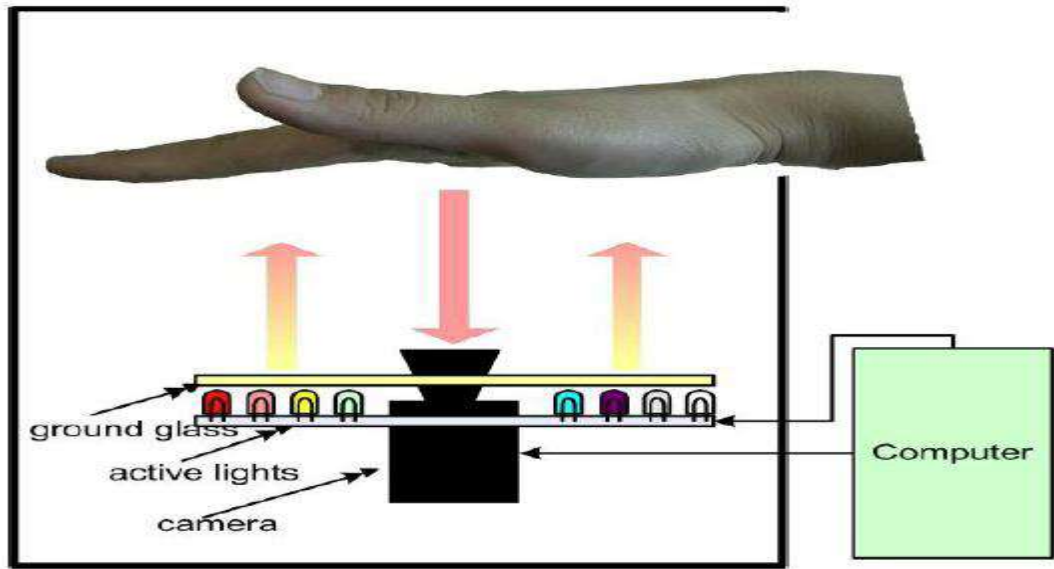


Fig. (0.1): Self-developed multi-spectral imaging device.

الخلاصة

القياسات الحيوية هي القياسات البيولوجية أو الخصائص الفيزيائية التي يمكن استخدامها لتحديد الأفراد. تلقي الأبحاث الحديثة الضوء على استخدام خوارزميات التصنيف في بيانات القياسات الحيوية لتطوير نظام جديد لتحديد الهوية أو آليات التحكم في الوصول. نظام يستخدم سمات القياسات الحيوية الفردية (عادةً صورة) ، والمعروف باسم نظام القياسات الحيوية أحادي الوسائط والذي يعتمد على ميزة واحدة لتحديد الهوية. لذلك ، تقترح هذه الرسالة نظام قياس بيولوجي أحادي الوسائط يستخدم بيانات القياسات الحيوية (التعرف على بصمة اليد) للتعرف على الأفراد. والغرض من هذا النظام هو بناء نظام قوي للتعرف البيومتري يستخدم عروق كف اليد كسمات. يتكون النظام من مرحلة المعالجة المسبقة لبيانات القياسات الحيوية ومرحلة التصنيف باستخدام الشبكات العصبية الالتفافية (CNN).

ولتحقيق هذا الهدف ، يلزم تصوير عروق كف اليد. يمكن التقاط عروق كف اليد اليدوية تحت جسم الإنسان باستخدام ضوء الأشعة تحت الحمراء (NIR) وضوء الطيف للكاميرا لالتقاطها. يجب أن تمر الصور بعدة مراحل مطلوبة للمعالجة المسبقة وهو أمر ضروري لإنتاج صورة واضحة لنمط عروق اليد اليدوية. يمكن بعد ذلك استخدام صور المخرجات لاستخراج الأنماط ومقارنتها بالخصائص المحددة لتحديد الأفراد بناءً على درجة التشابه.

يجب أن تُظهر الصورة المكررة بعد خطوات المعالجة المسبقة منطقة الاهتمام (ROI) التي توفر البيانات المفيدة المطلوبة لعمليات التدريب والمطابقة ، ومن ثم تم اقتراح خوارزمية لمنطقة الاهتمام. ستقوم الخوارزمية باستخراج النموذج عن طريق إزالة حدود راحة اليد أولاً وفصلها عن وريد النمط بحيث لا يمكن اتهام النظام بحقيقة أن الحدود جزء من الوريد. بعد استخراج منطقة الاهتمام ، تطبيق عدد قليل من مرشحات الصور ، مثل حالة المرشح المتوسط ، والمرشح متباين الخواص ، ونظام التشغيل الإغلاق مع إزالة الخلفية

للسماح باستخراج الأوردة بشكل واضح وتسهيل مهمة نموذج CNN. وبالتالي ، سيأخذ نموذج CNN نتائج مخرجات المعالجة المسبقة لأداء استخراج الميزة والمطابقة واتخاذ القرار. يشتمل النموذج على طبقة إدخال وطبقات مخفية وطبقة إخراج. تتضمن الطبقات المخفية طبقات الالتفاف ، والتي تلعب دورها في استخراج الميزات وإنتاج خريطة الميزات ، وطبقات تسوية الدفعات لتسريع عملية التدريب ، و ReLU لطبقات التنشيط.

تم استخدام قاعدة بيانات CASIA لصور عروق اليد في هذه الرسالة. يحتوي على 7200 صورة تم التقاطها لـ 100 شخص في ستة أطراف موجية مختلفة ، وهي 900 نانومتر ، 850 نانومتر ، 700 نانومتر ، 630 نانومتر ، 460 نانومتر ، واللون الأبيض. كل شخص في قاعدة البيانات لديه 12 صورة (كل يد 6 صور) لكل طيف موجي. وبالتالي ، تحتوي كل فرقة على 600 صورة لليد اليسرى و 600 صورة لليد اليمنى. تم استخدام مجموعة البيانات بأكملها. تم تقسيم الصور إلى تدريب واختبار بثلاث نسب مختلفة 50/50 و 30/70 و 10/90 للتدريب والاختبار على التوالي.

بينت النتائج أن الدقة الأعلى كانت بموجة من الطيف 850 نانومتر لأنها تمتلك الطول الموجي المثالي لاستخراج الأوردة ، وبالتالي فهي تساعد في تطوير نموذج دقيق. كانت الدقة بالنسبة لعروق اليد اليسرى 97% ، 97.5% ، 98% . وعروق كف اليد اليمنى 96% ، 97% ، 99% حسب نسب التدريب / الاختبار المقسم 50/50 ، 30/70 ، 10/90 على التوالي. تمت مقارنة نتائج النموذج المقترح بنتائج AlexNet وهي شبكة عالمية معروفة جيداً تم تدريبها على أكثر من مليون صورة ؛ لقد تفوق النموذج المقترح من حيث الدقة والوقت.



جمهورية العراق
وزارة التعليم العالي والبحث العلمي
جامعة القادسية كلية علوم الحاسوب وتكنولوجيا المعلومات

نظام تحديد وريد الكف بناءً على الشبكة العصبية الالتفافية

رسالة
مقدمة إلى مجلس كلية علوم الحاسوب وتكنولوجيا المعلومات بجامعة القادسية في
استيفاء جزئي لمتطلبات درجة الماجستير في علوم الحاسوب

من قبل

علي سلام حميد

بإشراف:

أ.م.د. علي محسن محمد